K.T. ERKILIÇ

EVALUATION OF THE THERMAL PERFORMANCE OF AUTOMOTIVE BRAKE DISC

THE GRADUATE SCHOOL OF NATURAL AND APPLIED SCIENCES
OF
ATILIM UNIVERSITY

KAAN TAMER ERKILIÇ

A MASTER OF SCIENCE
IN
THE DEPARTMENT OF MECHANICAL ENGINEERING

JANUARY 2023

ATILIM UNIVERSITY 2023

EVALUATION OF THE THERMAL PERFORMANCE OF AUTOMOTIVE BRAKE DISC

A THESIS SUBMITTED TO
THE GRADUATE SCHOOL OF NATURAL AND APPLIED SCIENCES
OF
ATILIM UNIVERSITY

BY

KAAN TAMER ERKILIÇ

IN PARTIAL FULFILLMENT OF THE REQUIREMENTS
FOR
THE DEGREE OF MASTER OF SCIENCE
IN
THE DEPARTMENT OF MECHANICAL ENGINEERING

JANUARY 2023

Approval of the Graduate School of Natural and Applied Sciences, Atılım University.

_____

Prof. Dr. Ender Keskinkılıç
Director

I certify that this thesis satisfies all the requirements as a thesis for the degree of **Master of Science in Mechanical Engineering, Atılım University**.

_____

Prof. Dr. Sadık Engin Kılıç
Head of Department

This is to certify that we have read the EVALUATION OF THE THERMAL PERFORMANCE OF AUTOMOTIVE BRAKE DISC submitted by KAAN TAMER ERKILIÇ and that in our opinion it is fully adequate, in scope and quality, as a thesis for the degree of Master of Science.

_____

Asst. Prof. Dr. Rahim Jafari
Supervisor

Examining Committee Members:

Asst. Prof. Dr. Ramin Barzegar
Department of Automotive Eng. Atılım University _____

Asst. Prof. Dr. Rahim Jafari
Department of Automotive Eng. Atılım University _____

Asst. Prof. Dr. Hamit Tekin
Mechanical Eng. Department, University of Turkish Aeronautical Association _____

Date: 13 January 2023

I hereby declare that all information in this document has been obtained and presented in accordance with academic rules and ethical conduct. I also declare that, as required by these rules and conduct, I have fully cited and referenced all material and results that are not original to this work.

Name, Last Name : Kaan Tamer ERKILIÇ

Signature :

ABSTRACT

EVALUATION OF THE THERMAL PERFORMANCE OF AUTOMOTIVE BRAKE DISC

ERKILIÇ, Kaan Tamer

MSc., Department of Mechanical Engineering

Supervisor: Rahim JAFARI

January 2023, **# 74**

Acceleration is a crucial dynamic for a vehicle, although deceleration is the key element for vehicle safety. A vehicle's braking system is the sole piece of equipment that can bring it to a slowdown or halt.

The function of a brake system is performed with the friction between disc and the pad. The thermal performance of the components it contains must be measured precisely in the design and test steps, and the component must show the required performance under operating conditions. In this study, an experimental setup was designed and produced to observe both aerodynamic and thermal characteristics of brake discs. Parts such as disc, pad, rim and tire on the experimental setup are exactly the same as those used in a typical passenger car. The quarter weight of a passenger car was adapted to the experimental setup on the shaft with cylindrical weights. In addition, a repetitive braking scenario was used in the experimental setup and simulations of the aerodynamic and thermal outputs of braking were carried out using detailed numerical models.

In the experiments and simulations, it was observed that the air flow caused by the acceleration of the vehicle reduced significantly inside the rim, despites there was a turbulent air flow that takes place with the form of eddies inside the rim. As a result of thermal simulations and experiments, the temperature distribution on the brake disc has been observed, and it has been predicted that the area where the brake disc contact

with the brake pad is higher than the temperature of the area directly opposite the contact area and the temperature is not uniformly distributed across the brake disc.

Keywords: *vehicle braking systems, active safety systems, vehicle safety systems, frictional heat, sequential braking*

ÖZ

OTOMOBİL FREN DİSKİNİN TERMAL PERFORMANSININ ÖLÇÜLMESİ

ERKILIÇ, Kaan Tamer
Yüksek Lisans, Makine Mühendisliği Bölümü
Danışman: Rahim JAFARI
Ocak 2023, **# 74**

Hızlanma bir araç için çok önemli bir dinamiktir, ancak yavaşlama araç güvenliği için kilit unsurdur. Fren sistemi otomobili yavaşlatacak veya durduracak en önemli ekipmandır.

Bir fren sisteminin işlevi, disk ve balatanın sürtünmesi ile gerçekleşir. İçerdiği komponentlerin tasarım ve test adımlarında ısıl performansları hassas bir şekilde ölçülmeli ve komponentin çalışma koşulları altında gereken performansı göstermesi gerekmektedir. Bu çalışmada, fren disklerinin hem aerodinamik hem de termal karakteristiklerinin gözlemleneceği bir deney düzeneği tasarlanmış ve üretilmiştir. Deney düzeneği üzerindeki disk, balata, jant ve lastik gibi parçalar tipik bir binek otomobilde kullanılanlar ile birebir aynıdır. Komponentlerle birlikte binek bir otomobilin çeyrek ağırlığı deney düzeneğine silindirik ağırlıklar yardımıyla şaft üzerine uyarlanmıştır. Bunun yanında, deney düzeneğinde tekrarlamalı fren senaryosu kullanılmış olup frenlemenin aerodinamik ve termal çıktılarının ayrıntılı numerik modeller kullanılarak simülasyonları gerçekleştirilmiştir.

Gerçekleştirilen deneyler ve simülasyonlarda, otomobilin hızı sebebiyle oluşan hava akışının jant içerisinde yavaşladığı ve buna rağmen jant içerisinde türbülanslı bir hava akışı olduğu gözlemlendi. Termal simülasyonlar ve deneyler sonucunda ise fren diski üzerindeki sıcaklık dağılımı gözlemlenmiş olup fren diskinin balata ile temas ettiği alanın temas alanının tam karşısındaki alanın sıcaklığına göre daha yüksek olduğu ve sıcaklığın eşit dağılmadığı tahmin edilmiştir.

Anahtar Kelimeler: *araç fren sistemleri, aktif güvenlik sistemleri, araç güvenlik sistemleri, sürtünme ısısı, tekrarlayan frenleme*

To My Beloved Family…

ACKNOWLEDGMENTS

I would like to thank Atılım University and its staff for their assistance and technical support.

I would also like to thank Rahim Jafari for giving me the chance for work on his projects.

I would like to thank Turkey Automobile Factory Inc. (TOFAŞ) and Scientific and Technological Research Council of Turkey (TÜBİTAK) for their financial support.

TABLE OF CONTENT

LIST OF FIGURES

FIGURES

LIST OF SYMBOLS

k	Thermal Conductivity, $W/(m \cdot K)$
k	Turbulent kinetic energy
m	Mass, Kg
m_{asp}	Surface roughness, asperities ratio
$\boldsymbol{n}$	Normal vector
p	Pressure, Pa
P	Kinetic energy, J
Q_f	Frictional heat, W
$\boldsymbol{q}$	Heat flux, W/m^2
q''_f	Frictional heat flux, W/m^2
T	Temperature, K
$\boldsymbol{u}$	Velocity vector, m/s
Greek Symbols	
μ	Dynamic viscosity, $Pa \cdot s$
	Coefficient of friction
ρ	Density, kg/m^3
σ	Stefan's constant, $W/(m^2 \cdot K^4)$
σ_{asp}	Surface roughness, asperities
	Height, m
ε	Turbulent dissipation rate, m^2/s^3
	Emissivity
γ	Heat partition factor
Subscripts	
d	Disc
p	Pad
avg	Average

CHAPTER 1
INTRODUCTION

This chapter serves as a detailed introduction to the project, including background information, basic braking knowledge, brake test methods and project motivation.

1.1 Background

Deceleration or stopping is as important as acceleration for a vehicle. This feature is an important safety factor for a vehicle that reaches high speeds and performs transportation. In this context, the design and performance of the braking system that performs deceleration or stopping is of great importance. Components of the braking system must be passed through certain testing stages while being designed.

These test stages are primarily carried out in the computer environment because it is inexpensive and fast. Finite element analysis and various Computational Fluid Dynamic programs are the first step in learning the necessary features of the design in terms of aerodynamic, thermal, and strength features.

After these parts are produced with the required features, they are tested in physical environments. As it is known, computerized analyzes can produce results close to real results, but what kind of behavior a component will show can only be obtained through real-world experiments. In this context, various test methods have been put forward to test the brake systems of automobiles. With these experiments, it can be observed how the components behave in the real world and what kind of properties they have.

1.2 Brake System Description

Today, brake systems in automobiles are commonly seen as disc brakes on the front wheels and drum brakes on the rear wheels. Some cars have disc brakes on all four wheels.

When a driver wants to slow down or stop the car, they press the brake pedal. The brake pedal transmits the hydraulic oil to the booster through channels. The booster increases the pressure coming from the driver's foot. Booster performs this pressure increase with a vacuum. This vacuum is generated from the intake manifold in internal combustion engines or with the help of a vacuum pump. The hydraulic oil with increased pressure coming out of the booster is transmitted to the master cylinder. The pressure force on the master cylinder coupled with the brake pads, which will contact the brake disc. The brake pads rubbing against the brake disc convert the vehicle's kinetic energy into thermal energy with the reaction from the driver's foot, thus slowing or stopping the vehicle.

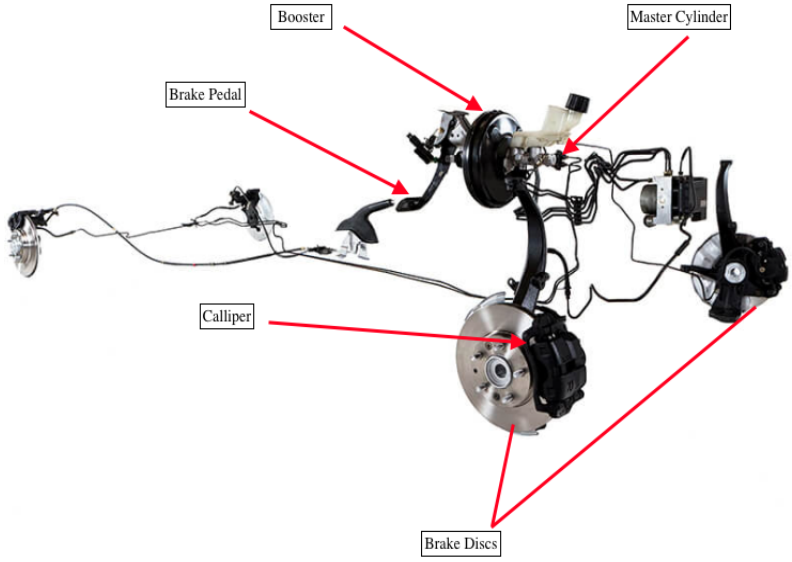

Figure 1.1: Brake system components location on a car taken and modified from Bendix (2022) [1]

1.2.1 Brake Disc

The brake disc or rotor is one of the parts that the car uses to convert kinetic energy into mechanical energy. This part, which is usually made of cast iron, is exposed to high force, friction, and very high temperatures.

As the name suggests, it is the main component of the disc brake system. Weight has become the most important factor for fuel consumption in automobiles. The concept called unsprung mass in vehicle dynamics refers to the load that the suspension does not carry, rather than the body weight of the car. One of the elements that make up this load is the brake disc. Reducing the unsprung mass has been observed to improve the driving dynamics and stability of vehicles. [2]

In today's cars, brake discs made of lighter materials are used as an alternative to heavy materials such as cast iron. The friction coefficients, thermal behaviors and cyclic lifetimes of these new materials are of great importance. The promising ones are aluminum alloys, titanium alloys, ceramic, and composite materials. [3]

Figure 1.2: Brake Disc. Taken from Brembo (2022) [4]

1.2.2 Brake Pad

Figure 1.3: Brake pads. Taken from Hella (2022) [5]

The brake pad is the part that makes friction by contacting the rotating disc. Two brake pads make contact with the surfaces of the rotor by means of hydraulic pressure. The increased hydraulic force from the driver's foot compresses the brake disc between the two pads. At the end of this compression, the kinetic energy of the brake disc is converted into mechanical energy through heat and the vehicle loses its speed.

The material of the brake pad is essential for braking. The most important feature sought in a brake pad is the high coefficient of friction between it and the brake disc. In addition, the wear characteristic of the material, its thermal performance and operational life are also important. In addition to this, environmentally friendly materials have been used in today's world where environmental factors increase their importance.

In the past, brake pad dust often released carcinogens such as asbestos into the environment. Today, asbestos brake pads have been replaced by pads called organic brake pads or non-asbestos brake pads. In addition, semi-metallic brake pads are also used. Semi-metallic brake pads are an inexpensive option that provides the required performance for large and heavy-duty vehicles. Another widely used material is ceramic brake pads. Ceramic brake pads have long life, high friction coefficient, low wear, and high thermal stress resistance, but they are expensive compared to other pads. [6]

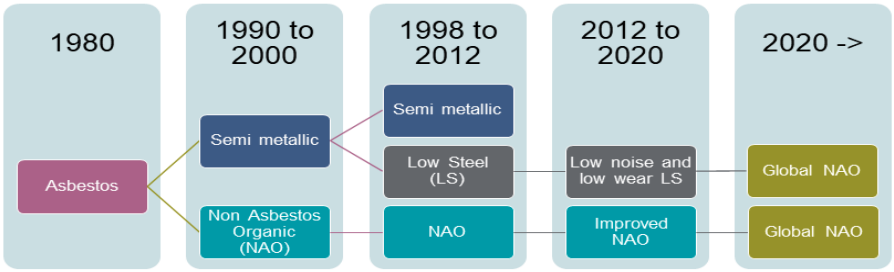

Figure 1.4: Automotive brake pad trend through the years. Taken from Lapinus (2022) [7]

1.2.3 Hydraulic System

Hydraulic system is one of the key components underneath the disc brake system. It transmits the force applied from the brake pedal through the rotor. The force applied by the driver will not be sufficient because the pressure force required to stop or slow down a car is very high. For this reason, it is necessary to increase the hydraulic pressure. As soon as the driver presses the brake pedal, it sends hydraulic oil to the booster (Power Brake). By increasing the pressure force coming to it, the booster sends the fluid to the master cylinder through the brake channels, and the master cylinder transmits the oil to the calipers. The calipers create the braking force by compressing the disc, creating the braking force that will stop or decelerate the vehicle.

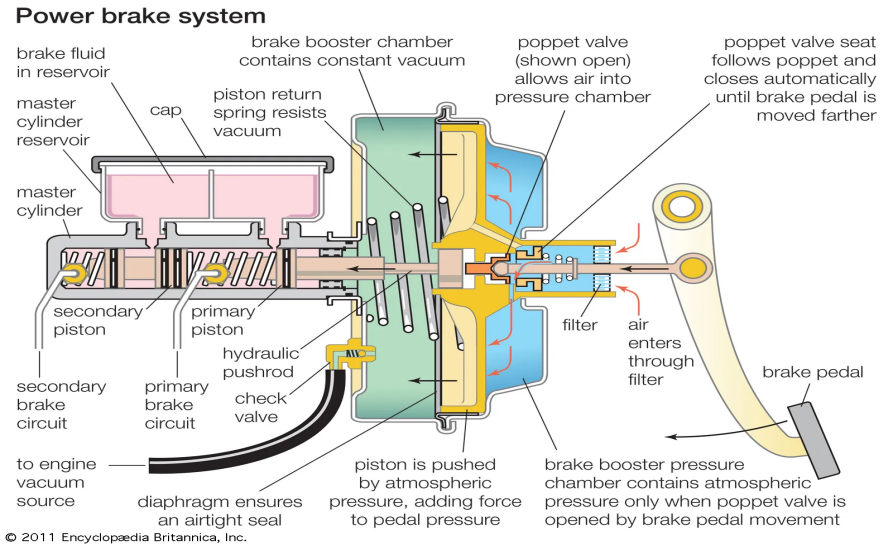

Figure 1.5: Booster (Power Brake) system taken from Britannica (2011) [8]

1.2.4 Brake Disc Aerodynamic Design

Figure 1.6: Brake disc types. Taken from Mew et. al. [9]

When brake discs convert kinetic energy into heat energy, a large amount of heat is generated as they are exposed to high frictional forces. This heat must somehow be discharged from the disc. Since the disc is a rotating part, it uses the air circulating around it for cooling. In order to use the air circulation more efficiently, engineers and researchers have adapted the vents or pins into the disc for their designs by using the centrifugal impeller theory on the brake rotor. Many disc variations with air channels have been produced, the main ones being radial vane, curved vane and pin-fin types. Research on this topic continues to find the most optimal design. In a study made with numerical analysis, the highest temperature of a ventilated brake disc was calculated 47 °C lower than a solid brake disc. Coulibaly et al. [10]. Jafari et. al. [11] developed 16 different ventilated disc models using the Taguchi method in his study. In this study, it was revealed that the ventilated gap is the most effective factor in cooling the disc.

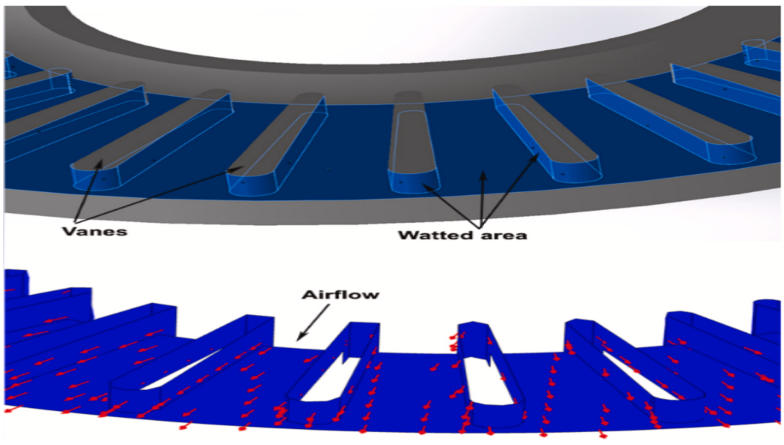

Figure 1.7: Ventilated brake disc with split part showing airflow passes through the vanes. Taken from Jafari et. al. [11]

1.3 Brake Disc Testing

Testing the reliability of the brake discs is an essential factor for the car's braking system. There are many methods for putting brake discs produced today to the test. One of the easiest and fastest ways is computer-aided engineering programs. In these programs, many features of a full-size brake disc such as frictional thermal properties, thermal stress resistance, service life, cooling performance of the brake disc and flow behavior of the air around the disc can be solved quickly by numerical methods.

Experiment setups are used to observe the compatibility of these simulations with real data. There are many different variations of these test setups. The most widely used of these are brake dynamometers, in which an AC motor mimics the motion of an automobile. In these brake dynamometers, first of all, the scenario in which the brake test will take place should be determined. These scenarios are either repeatedly accelerating and then stopping the brake disc or rotating the brake disc under a constant brake force. Parameters such as brake force and rotational speed of the brake rotor are important in these tests. The data to be measured in dynamometers is usually the temperature of the brake disc. Brake disc temperature is the only data that will reveal the thermal properties of the brake disc in these tests. Usually, in dynamometers, the

brake disc is accelerated and stopped by itself, but in the case of a car braking, the weight of the car on the tested brake disc is also a feature to be considered. The reason for this is that the produced disc must meet the required qualifications according to the vehicle variations in which it will be used. The brake dynamometer produced in this study was made by taking this detail into account. In addition, in some test setups, brake discs are scaled and tested. This is because dynamometers are expensive and take a lot of time to produce. Small scale dynamometers or tribometer devices are used because the scaled brake disc and brake pads are to be imitated as if they were on an automobile. Tribometer devices measure the friction coefficient and friction force between the brake disc and brake pad in contact. In brake disc test setups, some experiments are on brake disc failure. These tests are done to test the limits of the brake disc. What is meant to be understood in these experiments is to observe the temperatures at which the brake disc and brake pad degrade.

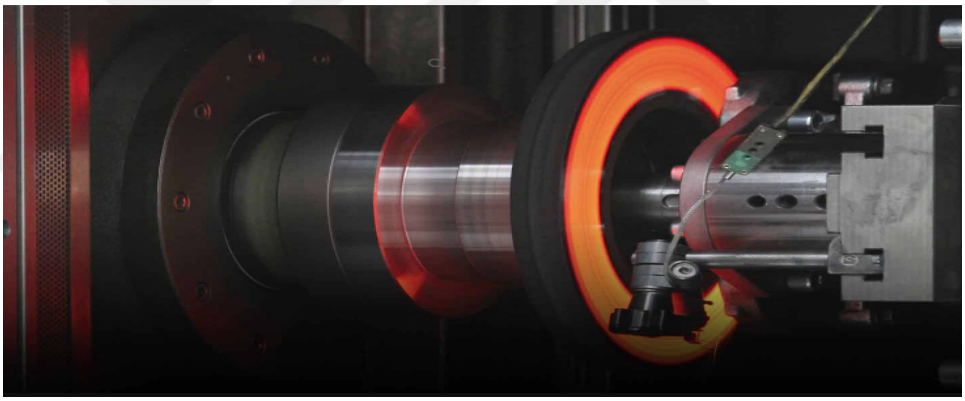

Figure 1.8: Overheated brake disc. Taken from Tecsa (2022) [12]

1.3.1 Thermal Judder

When the brake discs deteriorate, the first thing observed is the change of form of the disc due to temperature. This condition is called thermal judder. Thermal judder occurs when the material of the brake disc becomes unstable due to temperature. This is because the brake disc is poorly designed.

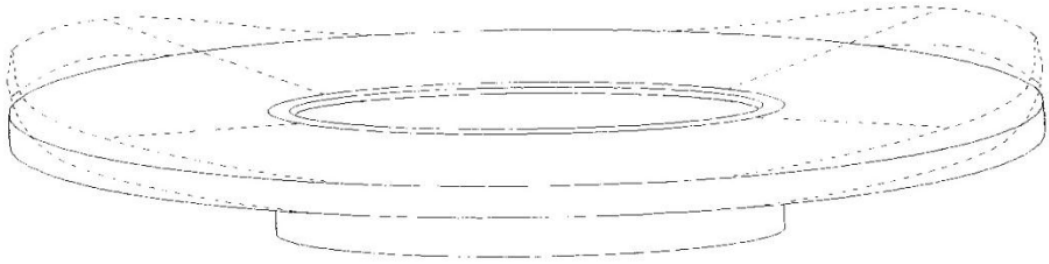

Figure 1.9: Butterfly effect due to thermal judder. Taken from Eggleston [13]

Figure 1.10: Coning effect due to thermal judder. Taken from Eggleston [13]

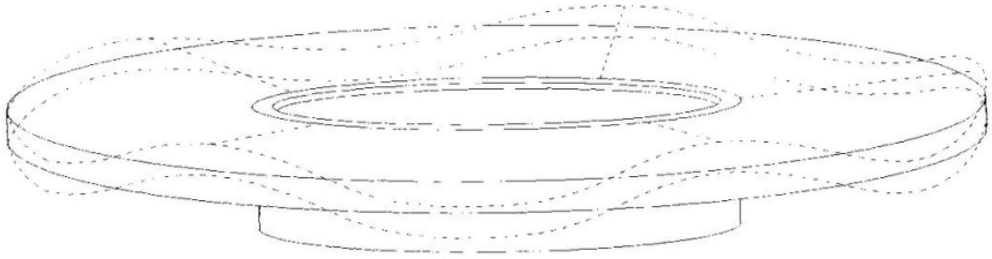

Figure 1.11: Corrugated effect due to thermal judder. Taken from Eggleston [13]

1.3.2 Thermal Cracks

At the same time, the brake disc is tested to produce cracks in these tests. The reason for the formation of cracks on the disc is that the temperature on the rotor is not uniformly distributed. The more the heated section on the disc surface tends to expand, as the lower temperature section cannot expand as much as the higher-temperature section, stress concentrations occur between these two sections on the disc surface. As a result of this situation, cracks occur on the disc. In order to overcome this problem, the thermal distribution of the brake disc must be well designed.

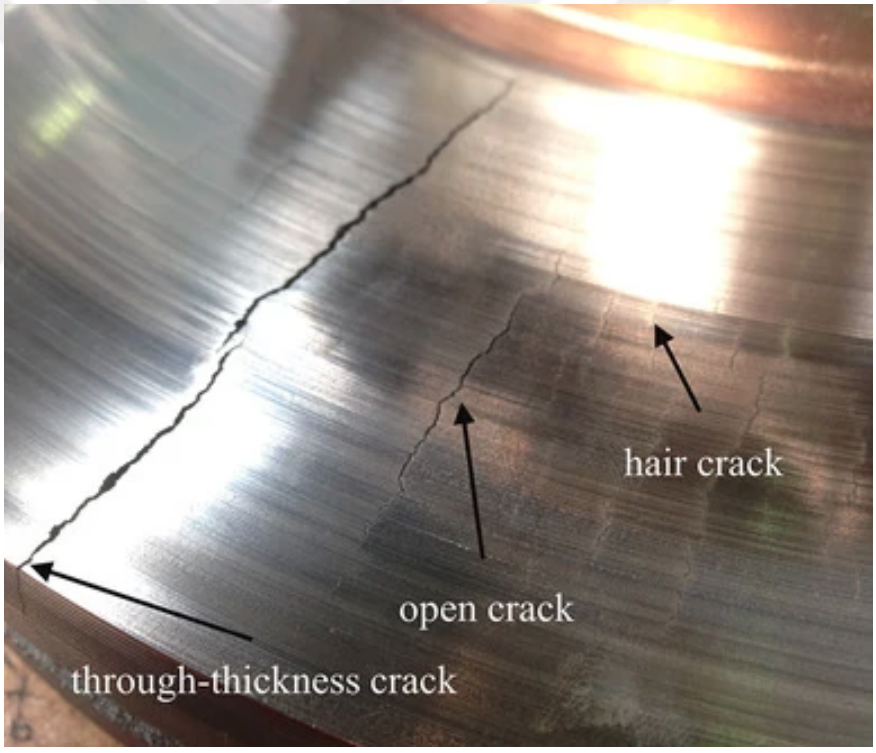

Figure 1.12: Crack types on brake rotor. Taken from Bilgic et. al. [14]

1.4 Literature Review

The kinetic and potential energies of the vehicle are converted into heat during braking by the frictional force between the disc and the pads. The heat generated by the friction force causes the disc and the pad's temperatures to increase. Brake vibration, thermal cracks and disc deformation, premature wear, and brake fluid evaporation are all effects of overheating in braking system components. The thermal performance of brake systems can be investigated in a variety of methods. Numerical models and experimental tests fall into two main categories of research techniques. Experimental braking experiments were conducted using on-road vehicle braking, brake dynamometer testing, and wind tunnel testing. Numerical models are preferred because of their low cost and detailed output. They can simulate a fracture of the brake rotor, entire disc, rotor and pads with boundaries and complete braking system.

1.4.1 On-Road Tests

One of the easiest ways to test brake performance would be to test each component separately from other components. Unfortunately, the brake system consists of many elements. Testing these components separately will result in different results as they work together with other components. Even if a test is performed in a laboratory environment with a complete braking system, it may produce different results from the real driving scenario.

There are two types of methods that test the performance of the brake system in real life conditions.

1. The first of these is the hill descent test (also known as the alpine descent). The first stage of the hill descent test takes place on a 10% slope from a high hill, when the car converts the potential and kinetic energy of its descent into heat with a constant braking force. This phase is called the warm-up phase.

In the second stage, which is called thermal soaking, the car going downhill is at a standstill. What is observed here is the heat that the brake rotor, brake pads and hydraulic system transfer to each other and to the environment.

2. The second test is “Auto Motor und Sport” (AMS) and it consists of 10 repeated cycles. In this test, at first the car accelerates to 130 km/h on a flat road, then its speed is reduced to 0 km/h with sudden braking. As a result of this action, the heat between the brake components of the stopped car and the environment is observed. It is also seen that during the Thermal soaking phase of some tests, the car does not brake and is driven at a constant speed while cooling off.

The drawback of road tests is that these tests cannot be performed continuously, and components cannot be fully tested due to unpredictable environmental conditions.

- Ambient temperature, humidity, and atmospheric pressure may differ from day to day. In the presence of these variables, the reliability of the tests decreases. In order to overcome these obstacles, it is necessary to constantly monitor the tested components while performing the tests.
- Another obstacle on-road tests is the wind factor. Since the direction and speed of the wind cannot be predicted, the effect of the wind greatly affects the components during the heat-up phase and the thermal soaking phase of the tests.
- Initial temperature changes are another factor affecting this test. While these tests are being carried out, different parts are tested, so installing them on a car that has completed several tests may have different results. To avoid this problem, the car needs to be brought to its initial condition, but this is time consuming and a factor that hinders repeatability.
- Another variable for this test is the driver. It cannot be expected that the drivers performing the tests will drive exactly the same as each other. Likewise, it differs in the ways in which the tests are carried out.

The coexistence of so many different variables can reduce the reliability of on-road tests, Vdovin et. al. [15]

1.4.2 Computational Simulations and Experimental Studies

Computational Fluid Dynamics Analysis method is another analysis method that measures the reliability of brake systems. In this method, brake components that are created in the computer environment and have real material properties are tested in the CFD program. These tests are in the form of simulations of the on-road tests mentioned in the previous section, but since the simulations are made on the computer, daily life variables can be easily eliminated from the calculations.

Schuetz et al. [16] compared the cooling process of the brake disc of the car in the CFD environment with the cooling process in the experimental environment.

In the simulations, thermal analyzes were made on the cooling times of the brake system by using the full-scale model of a car, including the brake system. Wind tunnel tests were carried out to validate the method after simulations in which the effects of the car's wheel movement in constant speed wind were taken into account and the effects of conduction and radiation were included. The methodology in the simulations was validated by comparing the average values of the brake disc cooling characteristic of the car obtained from the simulations with the average values of the cooling characteristics obtained in the experiments performed in the wind tunnel.

Vdovin et al. [17] developed an approach that combines aerodynamic and thermal codes in his study based on the downhill method for braking system tests. The wind tunnel test was carried out for validating the simulations carried out in the computer environment. Instead of calculating convection, conduction and radiation values in simulations performed on a full-scale automobile model, it embedded the convective heat transfer value calculated with aerodynamic codes into the conduction and radiation value of the brake system in the thermal code. The obtained results were used to recalculate convection and radiation.

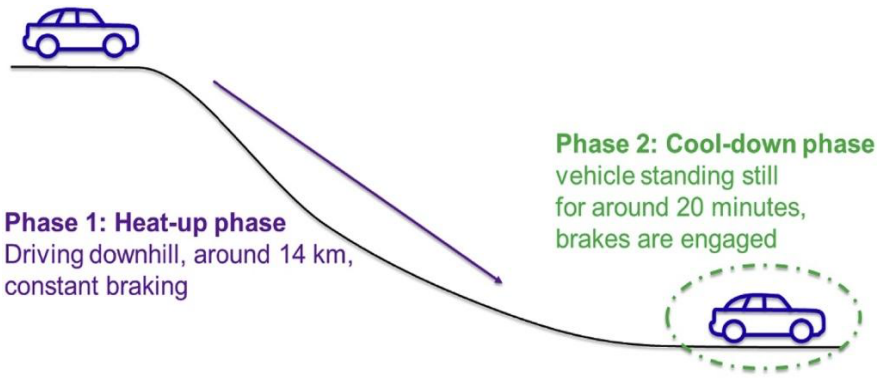

Figure 1.13: An Illustration of AMS downhill brake test. Taken from Vdovin et. al. [17]

Pevec et al. [18] used a ventilated brake disc in the simulations, only a part of this disc was used and the disc wall heat transfer constant and brake disc temperature were calculated at all speeds.

Experiments were carried out on the dynamometer to verify the results obtained. Performing an imitation of the AMS brake test, the dynamometer worked without the vehicle load by simply accelerating the brake disc. Temperature measurement from the middle part of the brake disc was made with a rubbing thermocouple. The reason for using the rubbing thermocouple is to accurately measure temperature while avoiding any stress concentration on the brake disc.

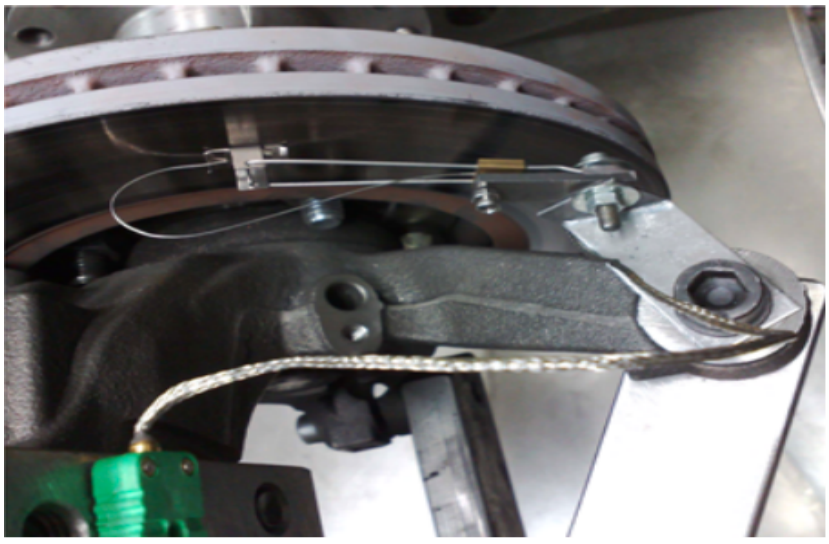

Figure 1.14: Rubbing Thermocouple on brake disc. Taken from Pevec et. al. [18]

Yan et al. [19] compared the standard brake disc with the cross-drilled ventilated brake disc in their study. In the comparison, firstly, CFD analysis was performed, and then the information obtained from the CFD analysis was verified in a specially designed experimental setup. In the CFD analysis part of the method used, only one sector of the brake disc and the surrounding air were considered. Constant volumetric heat generation is assigned to both friction surfaces of the rotor.

The test rig used in this study does not contain any caliper. The brake disc, which is connected to the AC motor with a shaft, is heated with the help of a heating pad, simulating the heat generated by friction. The rotational speed of the brake disc is controlled by an inverter connected to an AC motor.

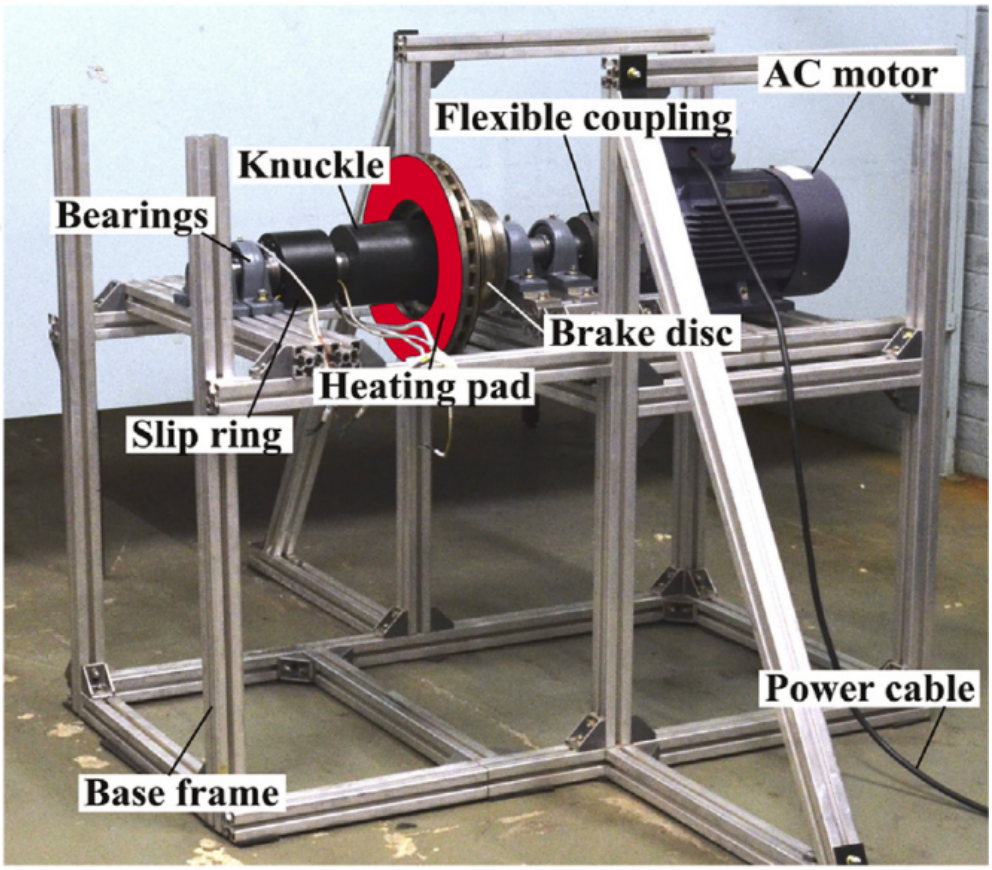

Figure 1.15: Brake disc test rig. Taken from Yan et. al. [19]

Shui et al. [20] modeled the brake disc and two brake pads with the finite element method in their article. In this study, a ventilated brake disc is used. The applied braking method is sequential AMS hard braking. In addition to analytical methods, experimental approaches take their place in the study. Flow correlations on the brake disc are used to calculate the coefficient of friction under boundary conditions. The radial and circumferential temperature changes were compared with the experiments performed on the brake dynamometer and verification was made. Temperature measurement was carried out with thermocouples embedded on the rotor in the brake dynamometer.

In another study, a numerical model was developed on the cooling behavior of the stationary brake disc in an environment where there is no air flow. This study is about how commonly used electronic parking brakes can provide better grip in a stationary car. The cooling behavior of the brake disc while the car is at a standstill has been investigated. To establish a numerical solution, a model based on the obtained analytical equations was used and tested at low rotational speeds where the temperature of the brake disc was increased evenly and uniformly by an induction heater to validate its data. After the tests, cooling of the stationary brake disc was observed. Tirovic et. al.[21] used a thermal rig and examined the disc surface by dividing it into rectangles and arcs. Rubbing thermocouple was used to read the temperatures.

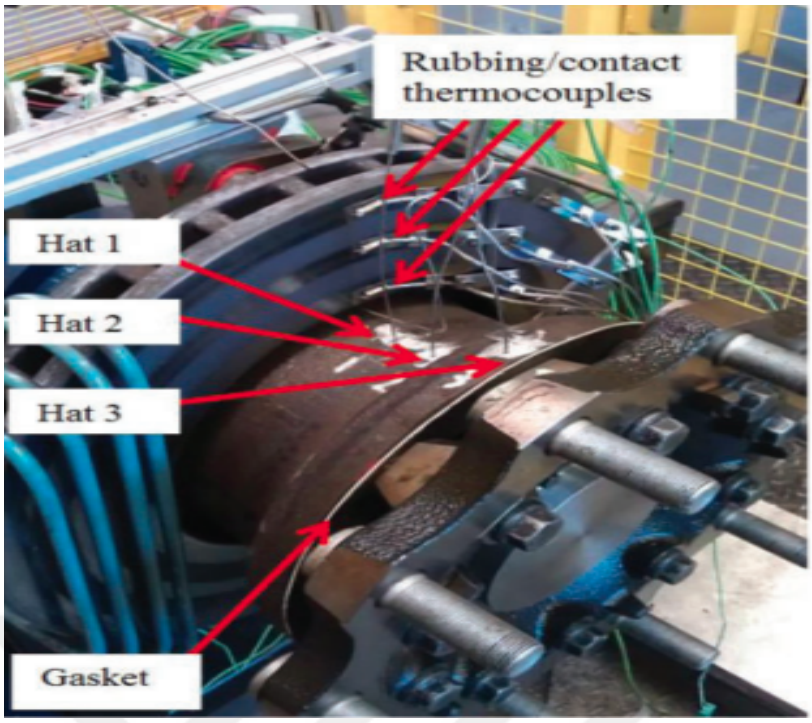

Figure 1.16: Thermal rig for brake disc and rubbing thermocouples. Taken from Tirovic et. al. [21]

Yevtushenko et. al. [22] came up with an iterative method based on Chichinadze's hypothesis to solve the nonlinear thermal limit of friction braking. In this study, the thermophysical properties of brake pad and brake disc materials were investigated. Using this model and the finite element method, Grzes et. al. [23] calculated the maximum temperature at the friction points where the brake disc and brake pad contact. Since this experiment will be a very sudden temperature change at the points with the highest temperature, it has not been experimentally tested in an experimental environment but has been carried out only with CFD analysis.

In another study, Grzes et. al. [24] performed a simulation with single braking for railway vehicles. A full-size brake rotor and brake pad were used for the experiments. In order to carry out the experiments more simply, a solid brake disc was used instead of a ventilated brake disc. The test setup used to compare the numerical results with the experimental results is the inertial test rig dynamometer, in which the brakes of the railway vehicles are tested.

Hwang and Wu [25] focused on temperature distributions and thermal stress in their research on brake discs. The brake disc used is a ventilated friction plate and a suitable brake pad. In the simulations and experiments, the single braking situation was taken into account, and the brake disc was subjected to friction with the help of brake pads until it lost its rotational speed. In the simulation, calculations were made considering the weight of the vehicle in which the brake disc is used. The axisymmetric 3d thermal model, which was used in CFD analysis by observing the thermal behavior of the brake disc reduced from 100 km/h to 0 km/h, was developed using approximate heat transfer coefficients within the boundary conditions.

Gigan et al. [26] performed repeated drag braking simulations and experiments on a full-size brake disc to better understand the thermomechanical loads on the brake discs. In the experiments using 8 different gray cast iron alloy discs, an embedded thermocouple was used to read the disc temperatures. The experiments were carried out on a full-size brake dynamometer. The main purpose of the study was to investigate the effect of the temperature produced on the brake disc on the life of the brake disc. The repeated drag braking scenario consisted of 1000 cycles and was carried out in 40 minutes. The reason why so many cycles are done in a short time is because thermal cracks are revealed quickly. In the experiment, the brake disc is accelerated at a speed of 80 km/h and braked until its speed drops to zero. According to the results of the dynamometer experiments, thermal loads on the disc cause the brake disc to plasticize and cracks tend to spread when the disc cools off.

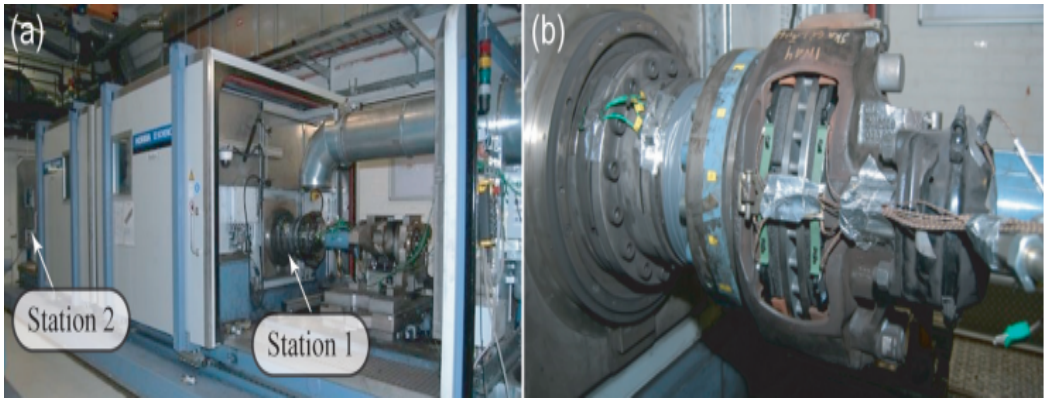

Figure 1.17: Overview of the full-scale brake dynamometer with stations 1 and 2; (b) close-up of the brake disc and caliper. Taken from Gigan et al. [26]

In another study on the brake disc, a 2d model was developed in which the thermal and friction properties on the contact conductivity on the disc surface were examined. Qui et al. [27] used a small-scale brake disc and brake pad. Temperature measurements were carried out with a rubbing thermocouple.

On the other hand, Abdullah [28], numerically found that the heat generation approach gives more accurate results than the heat partitioning approach for solving thermal problems in multi engagement.

Voller et al. [29] used CFD and Finite element methods in their numerical analysis in the cooling characteristic of brake disc research study and verified the data obtained from computer aided analysis by connecting test samples to the spin rig mechanism. In the spin rig experiment setup, the thermal contact resistance between the brake disc and the wheel carrier is precisely measured. In addition, the temperature of the disc and the wheel carrier were obtained with the embedded and rubbing thermocouples. The braking scenario used in the simulations is drag braking. The brake rotor performed rotational movement under a continuous braking force, but in these experiments, the brake rotor heated electrically. Since the focus of this study is to measure the cooling characteristic of the brake disc, it is not necessary to use the parts that perform the friction in the experimental setup. Spin rig only gave rotational speed to the disk and the disk was accelerated in the range of 40-450 rpm in the experiments. The results obtained showed that convection was the dominant heat transfer method and estimated that it had a share of 57% in the total heat transfer.

Hwang [30] conducted research on the temperature distribution on the disc, thermal distortion and thermal stress. This numerical study followed a repetitive braking scenario by reducing the brake disc from 100 km/h to 50 km/h. As a result of the simulations, Hwang estimated that the temperature distribution on the disc is in a non-uniform characteristic due to the variable heat flux in the contact area of the disc and brake pad and the heat dissipation in the areas of the disc that do not contact the pad.

Stojanovic [31] focused on the heat developed by contact pressure on the disc. In the numerical study, simulations were performed in three different variations by using different clamping pressures with a single braking method instead of a repetitive one. Disc temperatures were measured at 159.95 ℃, 175.3 ℃ and 190.62 ℃, respectively,

during braking with 0.9 MPa, 1 MPa and 1.1 MPa. Braking times in these simulations are a constant of 1,337 seconds. As a result of the study, the effect of contact pressure on temperature has been observed.

Galindo-Lopez [32] focused on the optimization of ventilated brake disc and heat dissipation in his doctoral thesis. The main purpose of this research is on the cooling characteristic of the brake disc. Lopez used a spin rig experimentally in addition to his numerical analysis. Since the focus of the study is the cooling characteristic, the heat on the brake disc is obtained by heating the brake rotor from the outside with an induction heater. Since the spin rig moves the disk rotationally, he preferred to measure the temperatures with a rubbing thermocouple.

Modanloo and Talaee [33] carried out their studies numerically. The aim of the study is to compare the cooling characteristics of solid and ventilated brake discs with simulations made at high speeds, and the analyzes were carried out in a CFD environment. As a result of the study, the solid brake disc reached 782°C as a result of braking, while the ventilated brake disc reached 659°C.

Jian et. al. [34] embedded heat pipes on the brake discs in his work. With 16 heat pipes embedded in the outer surface of the disc in rotational direction, it is aimed to increase the cooling performance of the rotor and a more uniform temperature distribution on the disc surface. As the braking scenario, he applied 15 consecutive braking and downhill methods in his experiments and simulations. In his results, he calculated that ventilated brake discs with embedded heat pipe had better temperature uniformity rates compared to ordinary ventilated brake discs, besides, brake discs with embedded heat pipe showed better cooling performance between 12.6% and 18.9%.

Figure 1.18: Embedded heat pipes on ventilated brake disc surface. Taken from Jian [34]

1.4.3 Reduced Scale Models

In studies using the reduced scale rule, a full-size brake disc is modeled and produced by scaling. A scaled imitation of the brake pad, which is the component that performs the friction, is also made with the same friction coefficient. Another consideration of this method used in testing brake discs is the applied braking force. In such experiments, a constant braking scenario is generally applied. As the dimensions are now reduced, the scaled brake disc is tested by connecting it to a high rpm tribometer. Tribometer is a device that measures the friction coefficient, wear, and friction force between parts.

In the light of the data collected in the studies so far, one of the problems encountered in experimental setups other than CFD analysis is the difficulty of measuring the temperature in a rotating metal alloy part. Since the brake disc is a metal part, measuring its temperature with infrared methods may result in affecting the sensitivity of the measuring device. On the other hand, a fixed thermocouple cannot be used during the experiment due to the rotational movement of the disc. The rubbing thermocouple used by Pevec et al. [18] is a cheap and practical method, but the effect of the heat generated by the surface of the thermocouple in contact with the disc on the test results should be considered. One of the disadvantages of a full-size test rig is that it is expensive and takes longer to manufacture due to its size.

Such difficulties were reported by Meresse et al. [35] and they followed a different method compared to other studies. In the study, the reduced scale rule was used. A full-size brake disc was modeled and produced to scale. The part that makes this method valid is that the brake disc produced by scaling is tested with elements that have the same friction coefficient as the full-size brake disc. Tested by connecting the scaled brake disc to the tribometer. The friction pin made the brake operation by contacting the disc during rotational movement. The heat produced on the disc was estimated from the inverse heat conduction and the temperature measurement was made with the telemetry system.

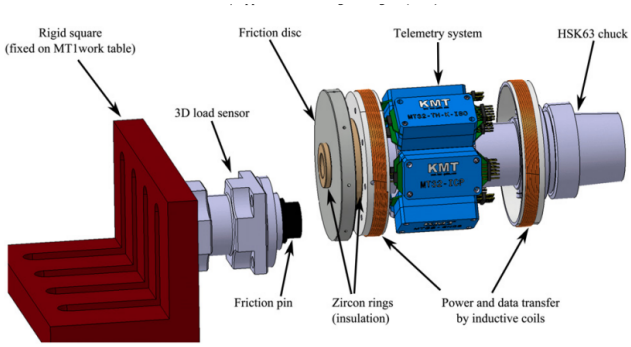

Figure 1.19: High speed tribometer schematic. Taken from Meresse et. al. [35]

Alnaqi et. al. [36] also resorted to the same method. In his work, he scaled and produced a full-scale brake disc. Experiments were made by connecting to the tribometer device with brake pads produced in the same scale. Rubbing thermocouple was used to measure the temperature of the brake disc in the experiments. Tribometer experiments served as a validation of the 2d simulations made. In order to ensure the accuracy of the tribometer data, dynamo experiments with a full-scale brake disc were performed according to the fixed braking scenario. As a result of the experiments, it was seen that the data obtained from the simulation were in good agreement with the tribometer experiments.

Sellami et. al. [37] analyzed the brake pad's contact with the brake disc thermally using the inverse method. After the convection parameters were solved in the numerical model, the results were compared with the tests performed on the tribometer device. If the difference in the results in the resulting overlap is more than the convergence threshold, the numerical model was minimized by the optimization method and the numerical model was updated. The method followed in this study was to produce a scaled brake disc using the reduce scale rule, and friction tests were carried out with a tribometer device. The temperature measurements of the scaled disc were made with a rubbing thermocouple.

In another of the studies on the brake disc, a 2d model was developed in which the thermal and friction properties on the contact conductivity on the disc surface were examined. Qui et al.'s [38] work uses a small-scale brake disc and brake pad. Temperature measurements were carried out with a rubbing thermocouple.

1.5 Project Motivation

The motivation of this study is to develop numerical and experimental methods that reveal low-cost and reliable results by determining the methods that will comprehensively analyze the brake discs that the domestic production TOFAŞ automobile factory will use in its automobiles in the future. In this study, on the designed or to be designed brake discs, it is desired to test the thermal behavior, aerodynamic properties, material performance of the brake disc with the help of computer aided programs and dynamometer.

1.6 Project Objectives

In the Introduction section, it is explained how the poorly designed brake discs fail due to the heat that is not uniformly distributed as a result of friction. Brake discs absorb kinetic energy in the form of conduction, convection and radiation. The aim of this study is to analyze these energy forms on the brake rotor correctly. In order to achieve this, the first thing to do is to create a fully accurate model of the brake disc to be tested in a computer environment and test it with computer-aided methods. However, the aim of this project is not only the performance of the brake disc, but also an analysis of the brake system formed by all brake components, both in the computer environment and in the experimental environment. For this reason, while modeling, the brake disc, brake caliper, brake pad, rim and tire of a mid-sized car will be modeled exactly the same sizes. In the experimental part of the project, an experimental setup with all the components will be designed, since it is desired to test the brake system of the car exactly. In this experimental setup, brake disc, brake pads, caliper, hub, booster, brake pedal and flywheel which will be used to simulate the inertia of the vehicle due to the load of the vehicle on the wheel of the vehicle to set up a complete brake system. In this setup, it was decided to use a rubbing thermocouple to obtain the temperature data on the disc. At the same time, the temperature values of the brake pads and brake fluid

will also be collected. Another data is the pressure of the brake fluid. Brake fluid pressure is the most important parameter to measure for braking force.

1.7 Project Limitations

It has been seen in the studies conducted so far that many methods have been developed to understand the behavior of brake discs, which exhibit complex behaviors in research processes. These methods include experimental results as well as computer aided analysis.

First of all, the air flow, which exhibits complex behavior in the wheel of the car, can lead to unpredictable results. In order to perform these analyzes precisely, turbulent air flow behaviors in CFD analyzes require large processor power.

One of the factors limiting the project is the force of the AC motor used in the dynamometer, which will imitate the movement of the car. The reason why a powerful motor is needed is because of the weight of the flywheels, which will mimic the inertia of the car's wheel. If the dynamometer cannot accelerate the disc fast enough, the disc will lose temperature during repeated braking.

Another limitation for this work is blowing fan’s air velocity. While this setup is based on the AMS hard braking scenario, air flow around the brake components should be simulated while testing. Due to this reason a blowing fan has been used to imitate air flow around the brake components. Unfortunately, blowing fans airflow speed is restricted to 17 m/s, which is not enough to generate flow speed around the components because components rotational motion is 105 km/h (29.61 m/s).

CHAPTER 2

THEORETICAL BEHAVIORS

In the previous sections, the practical behavior of the brake system has been explained. In this section, the braking behavior's dynamic and thermal background will be examined theoretically and mathematically.

2.1 Heat Generation

The braking system converts the kinetic energy of the vehicle into heat energy in order to decelerate or stop the speed of the vehicle. This heat transformation takes place at the contact surfaces between the brake disc and the brake pad. Energy transfer in the brake system is generally considered on surfaces where friction occurs. When braking, the brake pads exert a force on the brake disc, which creates a resisting torque in the opposite direction of the inertia of the wheel. This resisting torque, which occurs with the braking force, converts the inertial energy of the wheel into heat and slows the rotational speed of the wheel as soon as it starts to show its effect. The slowing wheel rotation speed creates a friction force in the area where the wheel touches the ground, which causes the speed of the car to slow down. In this transient phase, the wheel deforms to create the frictional force with the ground. This causes the accumulation of elastic energy in the tire. In addition, some of the elastic energy is absorbed in the chassis and suspension of the car. Therefore, it should not be sought to mean that the heat generated in the brake disc is directly equal to the reduction of the speed of the car. Another noteworthy situation is the slip behavior observed in the wheels of the car in case of high-force braking. Heat generation occurs as a result of slip that takes place in the contact area between the tire and the ground. However, considering a normal braking situation, the heat generation mentioned should be ignored alongside the amount of heat generated by the brake disc and brake pads.

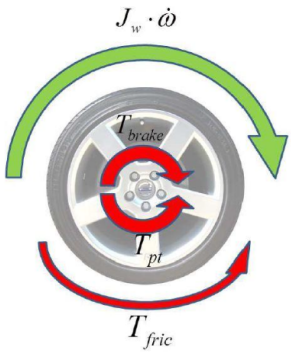

Figure 2.1: Torque balance overview on wheel. Taken from Neys [39]

Figure 2.1 above defines the following equation. The brake pads apply braking torque to the brake disc, and the brake disc reacts to this torque, creating a torque in the opposite direction, while the frictional force from the ground creates a torque against the inertia of the wheel.

$$J_w \cdot \dot{\omega} = T_{brake} - T_{fric} - T_{pad} \quad \text{(Eqn. 2.1)}$$

The torque character of braking is expressed as seen in the (Eqn. 2.1) above. When the dynamic behavior of braking is examined, the main subject of heat generation is the contact of the brake pads with the brake disc. In this case, the disc-pad heat energy should be examined with the following (Eqn. 2.2), (Eqn. 2.3) and (Eqn. 2.4.) Taken from Neys [39].

$$\dot{Q} = F_{friction} \cdot v_{slide} \quad \text{(Eqn. 2.2)}$$

Or:

$$\dot{Q} = T_{brake} \cdot \omega \quad \text{(Eqn. 2.3)}$$

Where:

$$T_{brake} = F_{friction} \cdot r_{eff} \quad \text{(Eqn. 2.4)}$$

2.2 Heat Dissipation

While the heat is built up in the brake disc and brake pad contact areas, there will be an immediate heat dissipation. The heat dissipation occurs brake pad-disc to the ambient air and other surrounding brake elements, including the brake fluid. Heat dissipation takes place in the form of conduction, convection, and radiation, see figure 2.2.

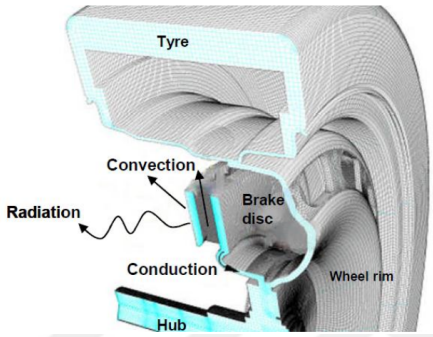

Figure 2.2: Heat transfer modes on brake components. Taken from Pulugundla [40]

2.2.1 Conduction

Thermal conduction, often known as heat conduction, is the heat transfer mode between solid particles. Typically described as λ, thermal conductivity is utilized as a material attribute for conducting (transferring) heat. A substance with a higher thermal conductivity transmits heat more rapidly than a substance with a lower thermal conductivity, as shown in (Eqn. 2.5) and figure 2.3 below.

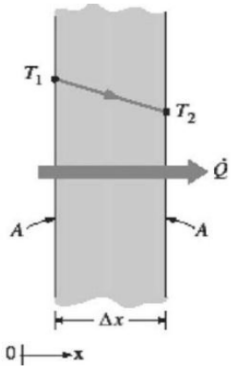

Figure 2.3: Illustration of thermal conductance. Taken from Thuresson [41]

$$\dot{Q}_{cond} = \frac{A \cdot \lambda \cdot (T_1 - T_2)}{\Delta x} = A \cdot \lambda \cdot \frac{\Delta T}{\Delta x} \quad \text{(Eqn. 2.5)}$$

Since conduction is a form of heat transfer that usually takes place between solid materials, in the brake system it occurs between parts with different temperatures. The heat generated by friction during braking is transmitted to the caliper that carries and moves the brake pads, and to the brake fluid hoses to which the caliper is connected. The heat in the brake disc is conducted (transferred) to the hubs and bolts that are carrying the disc. At the same time, the pistons of the caliper and brake fluid, which provide the movement of the brake pads, absorb the heat generated from the discs and pads.

2.2.2 Convection

Thermal convection or convective heat transfer is the behavior of heat transfer by moving fluids that transfers heat from one substance to another substance. This heat transfer mode is the main actor of heat transportation in the braking situation. According to Newton, this phenomenon is explained as (Eqn. 2.6) below, taken from Bergman [42].

$$\dot{Q} = h_{avg} \cdot A \cdot (T_1 - T_2) = h \cdot A \cdot \Delta T \quad \text{(Eqn. 2.6)}$$

Where:

$$h_{avg} = \frac{1}{A} \int h \cdot dA \quad \text{(Eqn. 2.7)}$$

As explained in the definition above, the convective heat transfer rate is dependent on the convective heat transfer coefficient, h, area and temperature difference. When braking occurs on the car that its velocity doesn't equal zero, generated heat transfers itself through surrounding air flow around the brake disc and pad. Air flow velocity generally increases the heat transfer rate. Also, the turbulence intensity around the brake disc usually increases the convective heat transfer.

2.2.3 Radiation

Another heat transfer mode that plays a role in the dissipation of heat in the brake system is radiation. Stefan-Boltzmann law (Eqn. 2.8) defines radiation below.

$$\dot{Q_{rad}} = \varepsilon \cdot \sigma_b \cdot A \cdot ({T_{obj}}^4 - {T_{env}}^4) \quad \text{(Eqn. 2.8)}$$

Which σ_b is Stefan Boltzmann's constant ($5.67 \cdot 10^{-8}$), ε is the emissivity ($0 \leq \varepsilon \leq 1$), A is the surface area, T_{obj} is the temperature of the object and T_{env} is the temperature of the surroundings.

In the light of this information, the heat generated on the disc as a result of braking is transferred to other components around the disc through radiation.

2.3. Pad And Disc Heat Distribution

In the light of the above information, the heat generated as a result of braking does not only distribute on the brake disc and brake pads. This heat is also absorbed by the brake components. Unabsorbed heat is dissipated to the air around the disc and pad by convection. Of course, the design of the braking system and environmental conditions will be a major factor in the distribution of this heat.

2.4. Cooldown Behavior

In the above sections, the generation of heat is examined. In this section, the cooling behavior of the brake disc will be explained

2.4.1. Mass Flow Rate

One of the most important factors in brake disc design is the mass flow rate. The most important feature in the design of the channels in the disc, which is explained in the aerodynamic design of the brake disc section in the Introduction section and helps the brake disc to cool, is the mass flow rate parameter. Since the disc is a rotating part, the heat around the disc is largely dissipated by convection.

The most effective cooling of the brake disc, which reaches high temperatures, is achieved with the help of ventilation channels in the rotor. The high mass flow rate significantly increases the cooling rate of a ventilated brake disc. Under this behavior, the brake rotor acts like a centrifugal impeller. The air in the channels is thrown out from the rotation center and creates a flow in the channels of the rotor.

2.4.2. Turbulent Flow

The form of the air flow around the brake disc is one of the most important factors in dissipating the heat produced by the disc and pad. The air inside the wheel flows with complex behaviors. The irregularity of this air flow is called turbulence. Turbulence is usually found in low viscosity fluids. Many unsteady developing eddy formations are seen in turbulence.

The higher the density of turbulent flow in the disc, the greater the amount of heat dissipated by convection. There are multiple ways to model turbulence in computational fluid mechanics programs. The turbulence model used in this study will be explained in the following sections. As figure 2.4 below turbulent flow behavior inside the wheel is modeled via COMSOL Multiphysics.

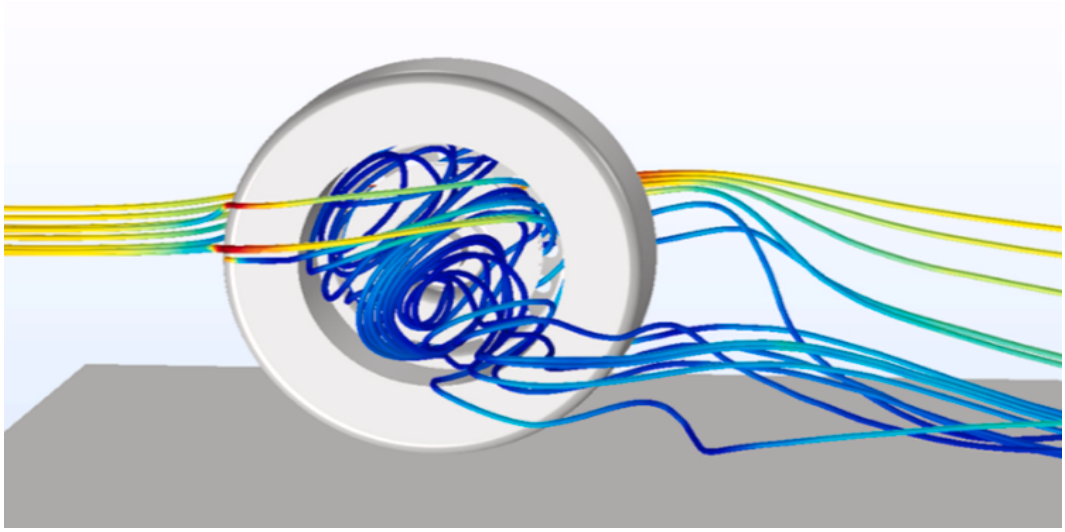

Figure 2.4: Turbulent flow inside the rim. Jafari [11]

CHAPTER 3

NUMERICAL MODEL

In this section, geometric, aerodynamic, and thermal models used in the computer aided engineering part of this study will be explained in detail. In this matter, Comsol Multiphysics used to develop thermal and aerodynamic simulations.

3.1 Brake Part Modeling

One of the main objectives of this study is to perform tests of a full-size brake system with all its components, both numerically and experimentally. In order to do this, first of all, the brake components planned to be tested in the experimental setup were modeled with their actual dimensions.

The wheel of a mid-sized passenger car and all the brake components in it are presented in fig 3.1 below. Knuckles, hubs and some unnecessary parts were excluded from the modeling in order to reduce the computation time and energy. The brake disc used in this model is a radial vane model.

Figure 3.1: Expanded view of brake components from left to right: tire, rim, caliper and pads, disc, dust shield, hub, knuckle.

Figure 3.2: Cross sectional view of modeled brake components.

3.2 Aerodynamic Model

One of the elements of the numerical model is the aerodynamic model. The aerodynamic model was developed to model the behavior of airflow around full-size modeled brake components in simulations and the effects of airflow on the thermal model of the brake disc.

Many different turbulence models are used to model the turbulent flow phenomenon, described in Theoretical Behavior section. The turbulence model used in the aerodynamic model in this study is $k-\varepsilon$. The $k-\varepsilon$ model is used alongside the Navier-Stokes equations. The k-ε model is based on solving two different variables. Where k is the kinetic energy of turbulence and ε is found to describe the dissipation of the kinetic energy of turbulence. Due to its high rate of convergence and somewhat low memory needs, the $k-\varepsilon$ model has historically been used extensively in industrial applications. It does not compute flow fields with jet flow, high flow

curvature, or unfavorable pressure gradients very correctly. For exterior flow issues involving complicated geometries, it does perform well.

Other turbulence models are more complex than the $k-\varepsilon$ model and without a reasonable initial prediction, they can frequently be challenging to converge. (Comsol.com)

An aerodynamic turbulent model has been assigned to calculate the velocity distributions, which is required to estimate the convection heat fluxes on the braking components. The well-known Navier-Stokes equations along with $k-\varepsilon$ turbulent model describe the velocity and pressure fields for the computational domain as follows

$$\rho\nabla\cdot(u)=0 \qquad \text{(Eqn. 3.1)}$$

$$\rho(u\cdot\nabla)u = \nabla\cdot[-pI+(\mu+\mu_T)(\nabla u+(\nabla u)^T)] \qquad \text{(Eqn. 3.2)}$$

$$\rho(u\cdot\nabla)k = \nabla\cdot\left[(\mu+\frac{\mu_T}{\sigma_k}\nabla k\right]+\mu_T[\nabla u:(\nabla u+(\nabla u)^T)]-\rho\varepsilon \qquad \text{(Eqn. 3.3)}$$

$$\rho(u\cdot\nabla)\varepsilon = \nabla\cdot\left[(\mu+\frac{\mu_T}{\sigma_\varepsilon}\nabla\varepsilon\right]+C_{\varepsilon1}\frac{\varepsilon}{k}\mu_T[\nabla u:(\nabla u+(\nabla u)^T)]-C_{\varepsilon2}\,\rho\frac{\varepsilon^2}{k} \qquad \text{(Eqn. 3.4)}$$

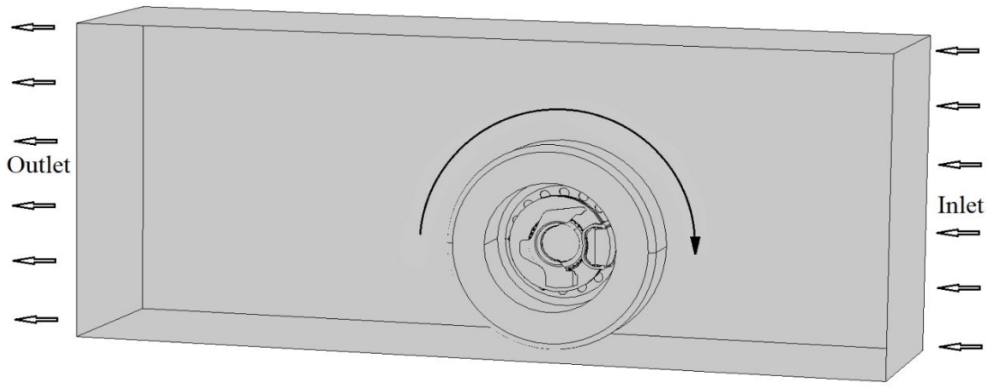

Figure 3.3: Computational domain including brake components.

Within the limits set for the aerodynamic model, the air enters the computational domain from the inlet and leaves the computational domain from the outlet, while passing through the gaps inside the brake components. As shown in Figure 3.3 above.

In order to focus the fluid motion in the computational domain to the brake components, slip wall boundary conditions are assigned to the side and upper walls of the domain. In this model, the tire, rim, hub and brake rotor are modeled as rotating walls, and the rotational speeds of these parts are adjusted proportionally to the speed of the wind entering the inlet, as in a real scenario.

The braking scenario used in the simulation is AMS hard braking. The wheel was first accelerated to 105 km/h, and then, with a sudden braking, it was reduced to 5 km/h in less than 2 seconds. The rotation speed of the dynamometer is set as 105 km/h in the experimental setup due to this scenario.

In this setup, flywheels weighing 1/4 of a mid-size car are connected to the shaft of the dynamometer in an axisymmetric position in order to simulate the inertia of the automobile wheel. Since this weight would make it difficult for the dynamometer to accelerate and the disc-pad temperatures would cool during this late acceleration, the dynamometer was adjusted to starting at 5 km/h, reaching 105 km/h, and then braking down to 5 km/h for 10 cycles.

Figure 3.4 shows the AMS brake test with ten successive cycles of acceleration and braking that is considered for the computational simulation.

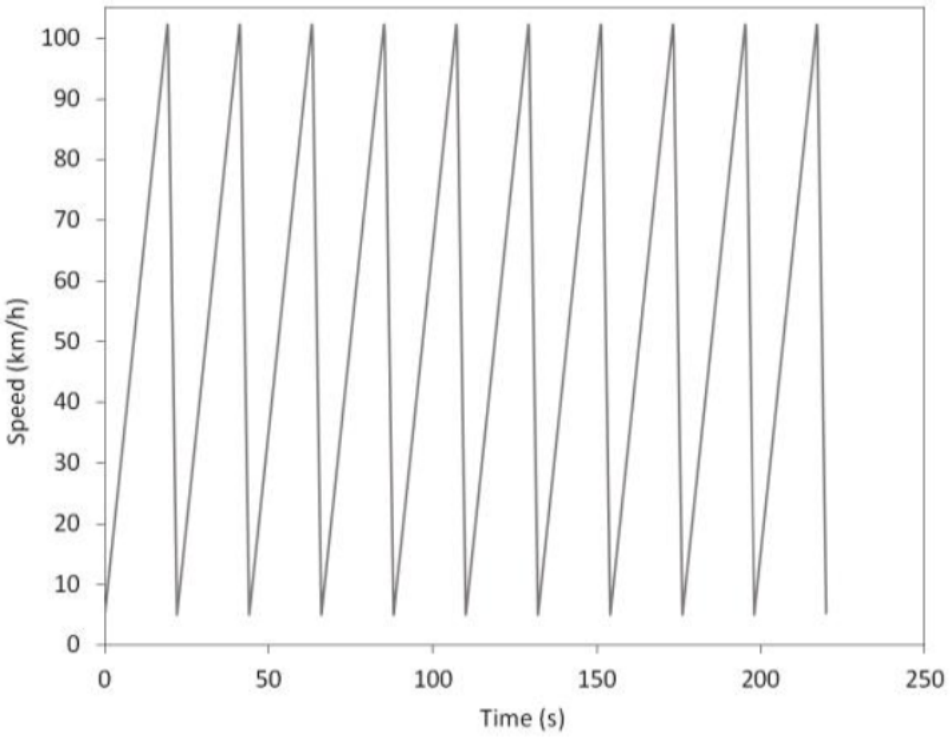

Figure 3.4 Speed variation for ten sequential braking at AMS hard braking test.

Figure 3.5 shows the acceleration and speed of the car used in the simulation in one cycle. Since it would take a long time to solve the transient turbulent flow with complex geometries in the computational fluid program, the problem in CFD has been solved in steady-state conditions.

As seen in Fig. 6, six steady velocities are used to approximately represent the velocity variations in the acceleration and deceleration sections.

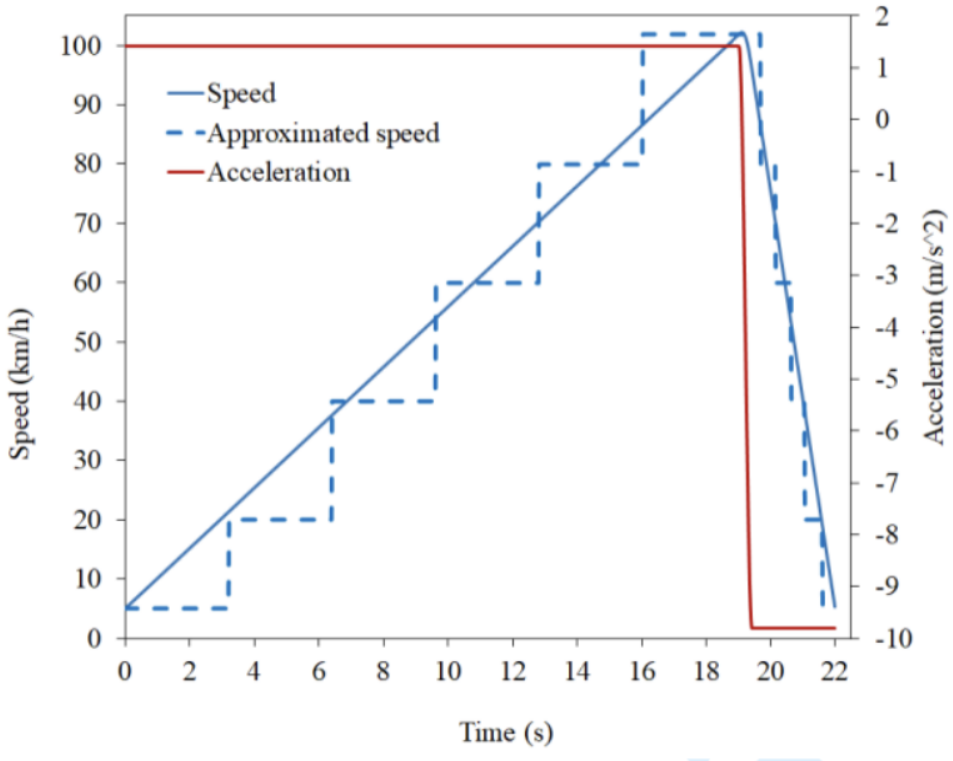

Figure 3.5: Speed and acceleration variations of a vehicle during one cycle of the AMS test.

3.3 Thermal Model

A thermal model has been developed to simulate the heat energy generated by friction in the brake system of the automobile. In this thermal model, the kinetic and potential energies of the passenger car are converted into thermal energy during braking by performing simulations in accordance with the AMS hard braking scenario. The potential energy is assumed to be zero in the simulation.

At the same time, the heat due to wear is neglected and only the heat due to friction between the brake disc and pad is included in the calculations of the thermal model.

Since the thermal energy develops between two sliding surfaces in contact with each other, it is necessary to make heat partition solutions of these surfaces (brake disc and brake pad). The heat partition equation is expressed as follows. In this (Eqn. 3.5), q_d and q_p denote heat flux at the disc and heat flux at the pad, respectively.

$$-n_d \cdot q_d = -h\left(T_p - T_d\right) + \gamma q''_f \quad \text{(Eqn. 3.5)}$$

$$-n_p \cdot q_p = -h\left(T_p - T_d\right) + (1 - \gamma) q''_f \quad \text{(Eqn. 3.6)}$$

γ is calculated from Charron's relation as

$$\gamma = \frac{\sqrt{\rho_d C_{p,d} k_d}}{\sqrt{\rho_d C_{p,d} k_d} + \sqrt{\rho_p C_{p,p} k_p}} \quad \text{(Eqn. 3.7)}$$

h is the joint conductance, which is written as

$$h = h_c + h_g + h_r \quad \text{(Eqn. 3.8)}$$

The gap conductance (h_g) is taken zero.

$h_r$is radiative conductance and is calculated as

$$h_r = \frac{\sigma \varepsilon_d \varepsilon_p}{\varepsilon_d + \varepsilon_p + \varepsilon_d \varepsilon_p} \left({T_d}^3 + {T_d}^2 T_p + {T_p}^2 T_d + {T_p}^3 \right) \quad \text{(Eqn. 3.9)}$$

Where σ is Stefan's constant, ε_d and ε_p are respectively emissivity of the disc and emissivity of the pad.

h_c is constriction conductance, which approximated by Cooper-Mikic-Yovanovich [43] correlation as

$$h_c = 1.25 k_{contact} \frac{m_{asp}}{\sigma_{asp}} \left(\frac{p}{H_c} \right)^{0.95} \quad \text{(Eqn. 3.10)}$$

Surface roughness properties of m_{asp} and σ_{asp} are respectively asperities average slope and height.

$K_{contact}$ is the harmonic mean of the contacting surface conductivities and calculated as

$$k_{contact} = \frac{2 k_d k_p}{k_d k_p} \quad \text{(Eqn. 3.11)}$$

The deceleration power of a brake is given as the negative of the time derivative of the vehicle's kinetic energy as

$$P = -\frac{d}{dt} \left(\frac{1}{2} m v^2 \right) = -mv \frac{dv}{dt} \quad \text{(Eqn. 3.12)}$$

Where m, v and $\frac{dv}{dt}$ are the vehicle's total mass, velocity, and deceleration, respectively.

The frictional heat flux at a contact area (A) between the disc and the pad is

$$Q''_f A = Q_f = -\frac{1}{8} mv \frac{dv}{dt} \quad \text{(Eqn. 3.13)}$$

For system with constant mass, the second law of Newton can be expressed as

$$F_f = -\frac{1}{8} m \frac{dv}{dt} \quad \text{(Eqn. 3.14)}$$

The frictional force value in (Eqn. 3.14) is substituted in (Eqn. 3.13) as

$$Q_f = F_f v \quad \text{(Eqn. 3.15)}$$

The frictional force at the contact area equals to

$$F_f = \mu F_n \quad \text{(Eqn. 3.16)}$$

Substituting the frictional force value obtained from (Eqn. 3.16) in the (Eqn. 3.15) gives

$$F_n = \frac{Q_f}{v\mu} \quad \text{(Eqn. 3.17)}$$

The normal force is proportional to the contact pressure and would be written as

$$F_n = pA \quad \text{(Eqn. 3.18)}$$

Substituting the value of the normal force obtained from (Eqn. 3.18) in the (Eqn. 3.17) gives

$$p = \frac{Q_f}{\mu v A} \quad \text{(Eqn. 3.19)}$$

In order to calculate transient temperature distribution in the computational domain, the heat equation for three-dimensional Cartesian coordinate is employed as

$$\rho C_p \frac{\partial T}{\partial t} + \rho C_p u \cdot \nabla T - \nabla \cdot (k \nabla T) = Q \quad \text{(Eqn. 3.20)}$$

3.4 Meshing and Computational Domain

When dealing with computational fluid dynamic programs, one of the things that should be done before starting the analysis is to partition the model into small cells after a computational domain is determined. This approach is called meshing. Mesh models can be in many different geometries. In this study, the mesh model used to perform the simulations is in tetrahedral geometry. The computational domain is 2 m long, 1m wide and 1m height to ensure that there is no unwanted interference from the domain boundary conditions. The braking parts are positioned 0.5 m far from the inlet shown in Figure 3.3 above. Domain is completely covered with a tetrahedral grid. Figure 3.6 shows the mesh assigned to the computational domain. In addition to the computational domain, the brake components in the domain are also partitioned into small cells with the same type of mesh.

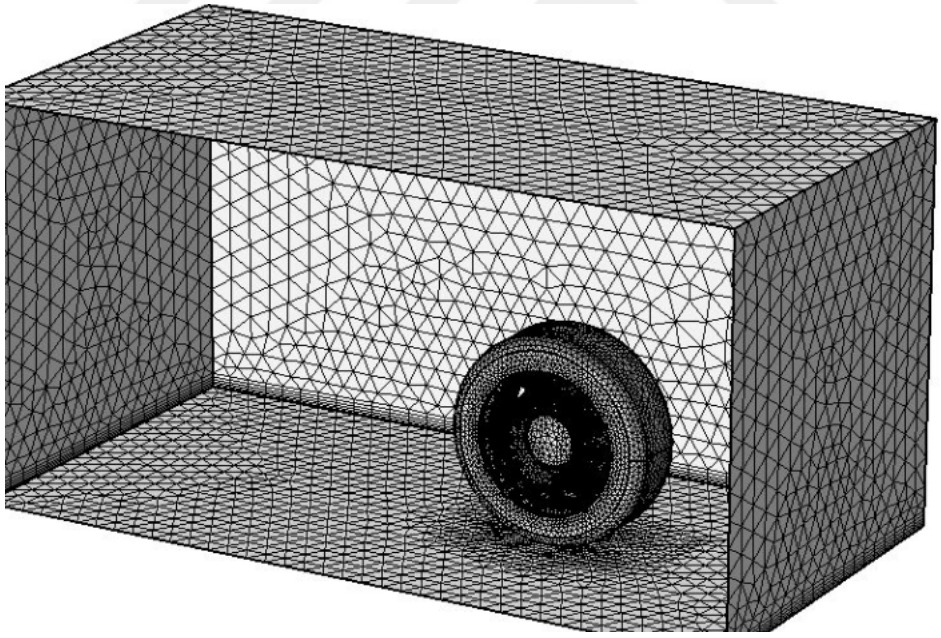

Figure 3.6: Meshed computational domain and brake components.

The feature that needs attention here is the quality of mesh. The size of the cells the mesh creates will affect the quality of the analysis and the computation time. Brake disc and brake pad are the focus of CFD analysis. Since parameters such as speed and temperature will be analyzed here, the quality of the mesh in these regions should be higher than the mesh quality of other components. For this reason, high resolution mesh is assigned to the brake disc and brake pad. Figure 3.7 shows the difference in resolution between the mesh assigned to the brake disc and brake pads and the mesh assigned to the other components.

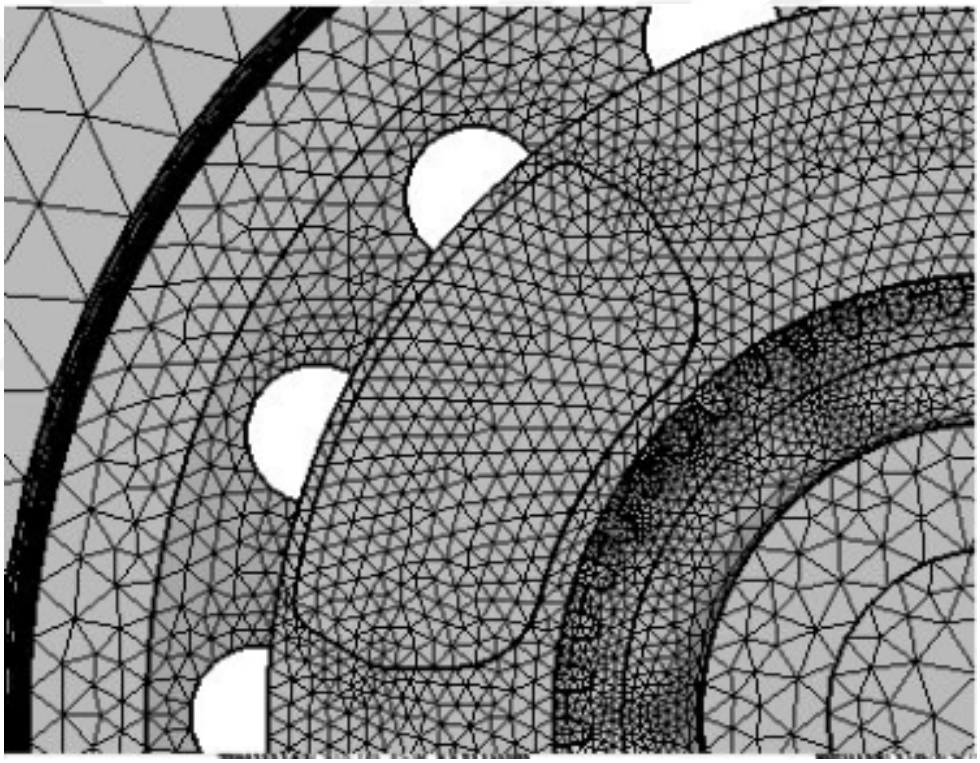

Figure 3.7: Mesh quality difference between disc-pad and other components.

In addition, good quality grids were applied to both sides of the brake disc with a thickness of 1mm. Shown in Figure 3.8.

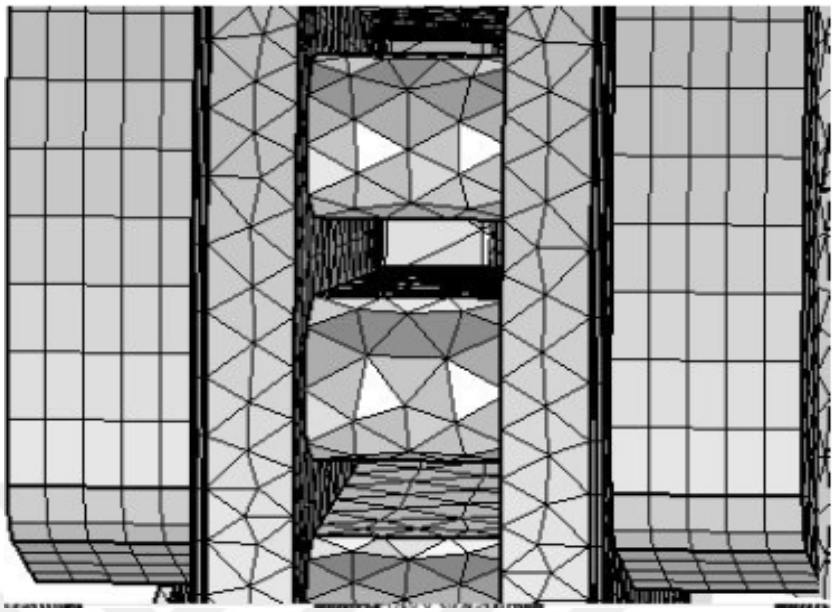

Figure 3.8: Grids on both sides of the brake disc.

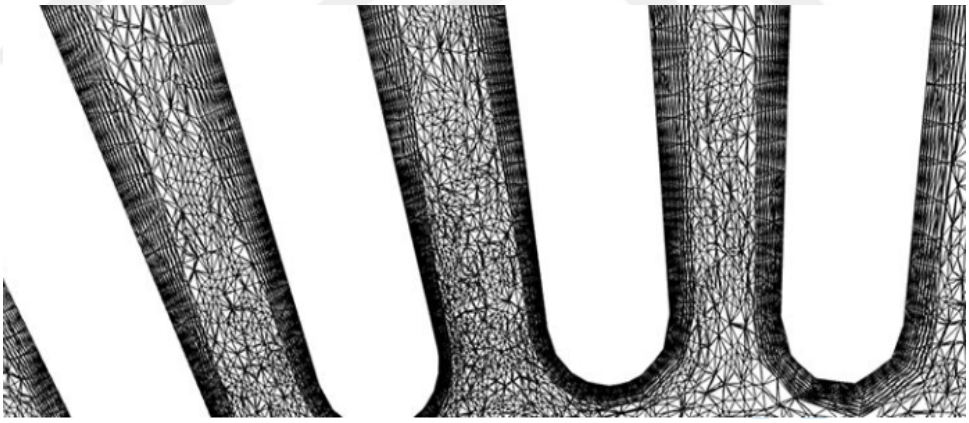

Figure 3.9: Mesh quality of radial fins on the disc.

To capture the boundary layers, prism layers were imposed on the walls as shown in above Figure 3.9 for the radial vanes.

In meshing the same volume mesh is used for both the aerodynamic and thermal simulations.

CHAPTER 4

SIMULATIONS

This part will explain simulation characteristics of the numerical model and the obtained simulation results.

4.1 Simulation Characteristics

The methodology prepared for the testing of full-size brake tools, which is the aim of the study, consists of two different steps, respectively, Simulation and Experiment. The first of these is the Simulation, which is solved numerical calculations and analyzes in computer-aided engineering programs. Firstly, the brake components are modeled with material properties in a SolidWorks 2018, a computational domain is determined after the material properties are assigned to the inputs in the thermal and aerodynamic model to be solved in the COMSOL Multiphysics simulation. In the thermal and aerodynamic simulations to be carried out in this domain, first the brake components of the car are positioned in the domain. Then the conditions for the simulation are determined. These conditions are within the capability limits of the experimental setup.

Since the experimental setup is capable of accelerating the wheel of the car to 100 km/h, the speed parameter in the simulation conditions was also set to 100 km/h. At the same time, the contact pressure between the disc and the brake in the experimental setup is the limiting factor for the simulation. In the experimental setup, 14 bars were measured for contact pressure between disc and pad. After the simulation conditions and limits are determined, the braking behavior to be simulated is assigned to the simulation. Since the scenario that is intended to be applied in the experimental setup is the AMS hard braking test, the data of the thermal and aerodynamic study of the brake parts will be obtained by the analyses made on this braking behavior for the simulation.

4.2 Simulation Results

The simulation results will be examined under two main headings as they include aerodynamic and thermal simulation data.

4.2.1 Aerodynamic Simulation

In this simulation, a detailed analysis of the air flow around the brake components is performed. In the aerodynamic simulation, the flow velocity distribution of the wind on the brake components and the behavior of the turbulent flow in the wheel data were collected by visualizing in the computational domain.

According to the results of the air flow around the wheel in aerodynamic simulation; the air flow drops to a level close to zero after it contacts the front of the wheel. The air flow accelerates around the shoulder of the wheel. The velocity of the airflow accelerated at the edge of the wheel exceeds the velocity of the inlet in the computational domain.

It has been observed in the analysis results that the air flow has lost its speed significantly inside the rim. While the speed of the air flow is 29 m/s at the inlet, it decreases to 11 m/s around the brake disc in the rim. The figure below 4.1 shows the distribution of airflow velocity in the computational domain.

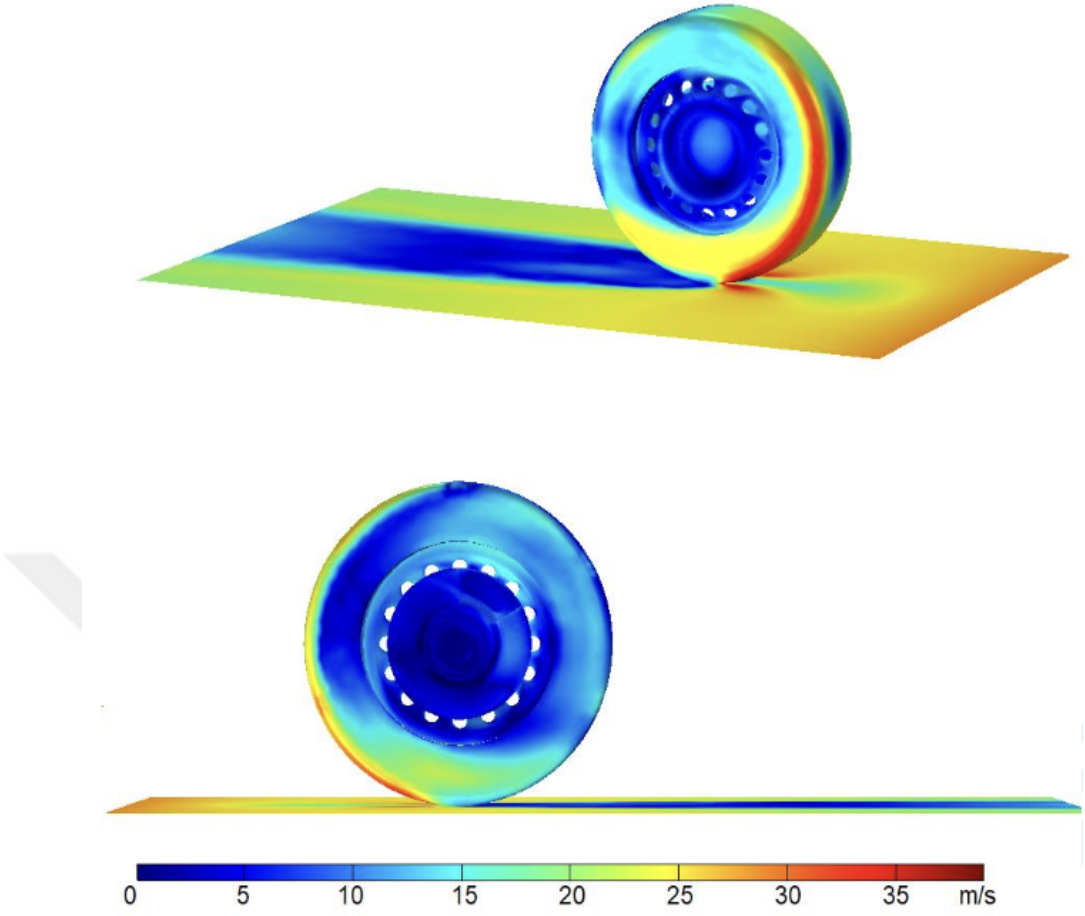

Figure 4.1: Airflow velocity distribution around the brake components.

In addition to the velocity distribution of the air around the brake components, turbulent flow formations in the rim are observed when the air flow is viewed as three-dimensional streamlines. Shown in Figure 4.2. As the wheel exhibits translational and rotational movements at the same time, a complex turbulent flow occurs within the rim. In Figure 4.3, streamlines are viewed from a cross sectional view. Streamlines at a distance of 5mm from the disc on the plane show that eddies of different intensities within the rim are formed in the swirling air flow. The number of these vortices, the positions they occur in, and their intensities can vary with variations in airflow velocity in the inlet of the computational domain. This aerodynamic simulation provides a comprehensive aerodynamic analysis of the air flow around the brake components. The flow behaviors, which are impossible to measure by experiments, are obtained by simulation.

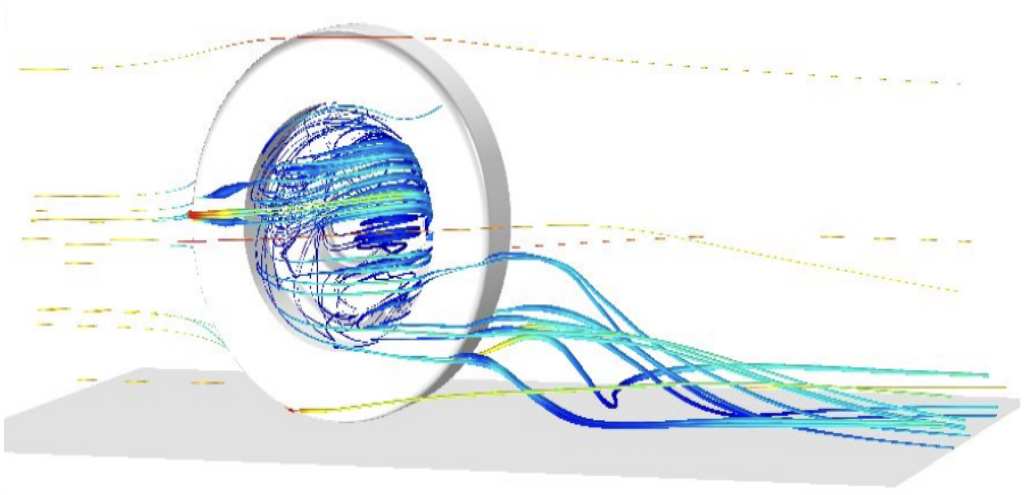

Figure 4.2: Streamlines distribution in computational domain.

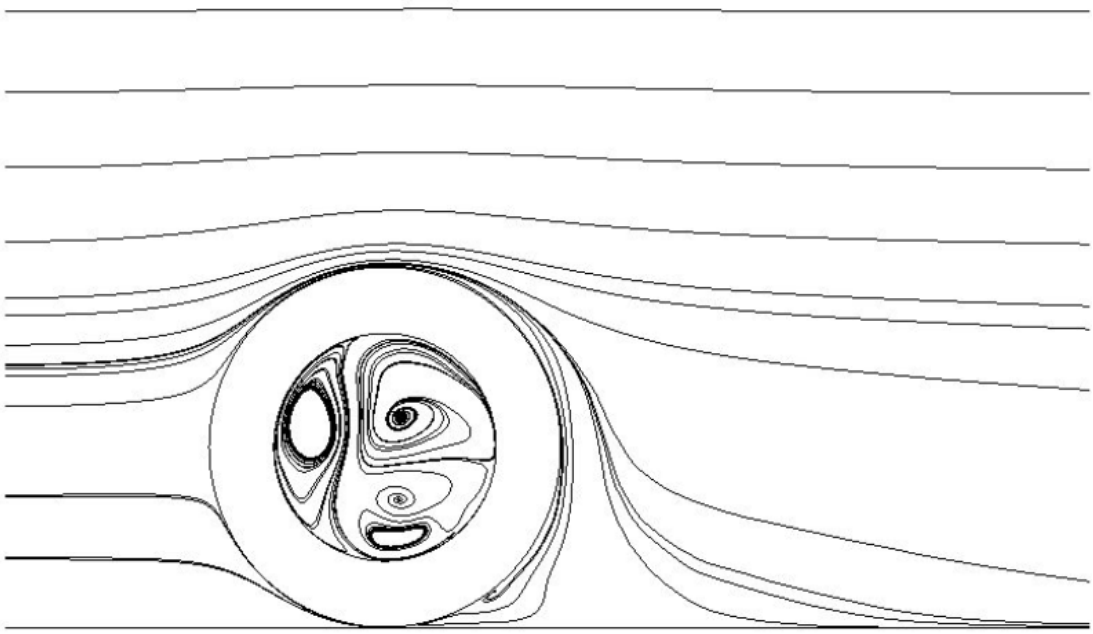

Figure 4.3: Streamlines inside rim with cross sectional view.

4.2.2 Thermal Simulation

As stated in the paragraph in the main title before, it has been mentioned that the parameters in the experimental setup are used to ensure the correlation of the simulation with the experiment. These parameters are rotation speed of the wheel, the contact pressure between the disc and the pad, parts dimensions and properties of the components which were used in the experimental test setup. Contact pressure is one of the important parameters for calculating the temperature generated by the friction of the disc and pad against each other. In addition to the contact pressure, the friction coefficient and contact area of the disc and brake pad are also important for thermal simulation.

The contact pressure is proportional to the heat generated by friction as expressed in (Eqn. 3.19). In addition, the friction coefficient, velocity and contact area in the equation exactly match the parts used in the experimental setup. Another role of contact pressure here will be the key factor in calculating frictional heat values to ensure consistency between experimental data and simulation data.

At the moment of braking in the test setup, the brake oil pressure increases in the master cylinder. Brake fluid reaches the caliper through the brake channels. With the increase in pressure in the oil, the pistons of the caliper press the brake pad towards the disc from both sides and braking occurs. A pressure sensor is connected to the master cylinder to measure the braking pressure formed here. The measured pressure value is used in the simulation.

Figure 4.4 below shows the contact pressure applied between the disc and pad in the simulation. The simulated pressure leaps sharply from zero bar to its maximum value of 14 bar, and then drops back to zero.

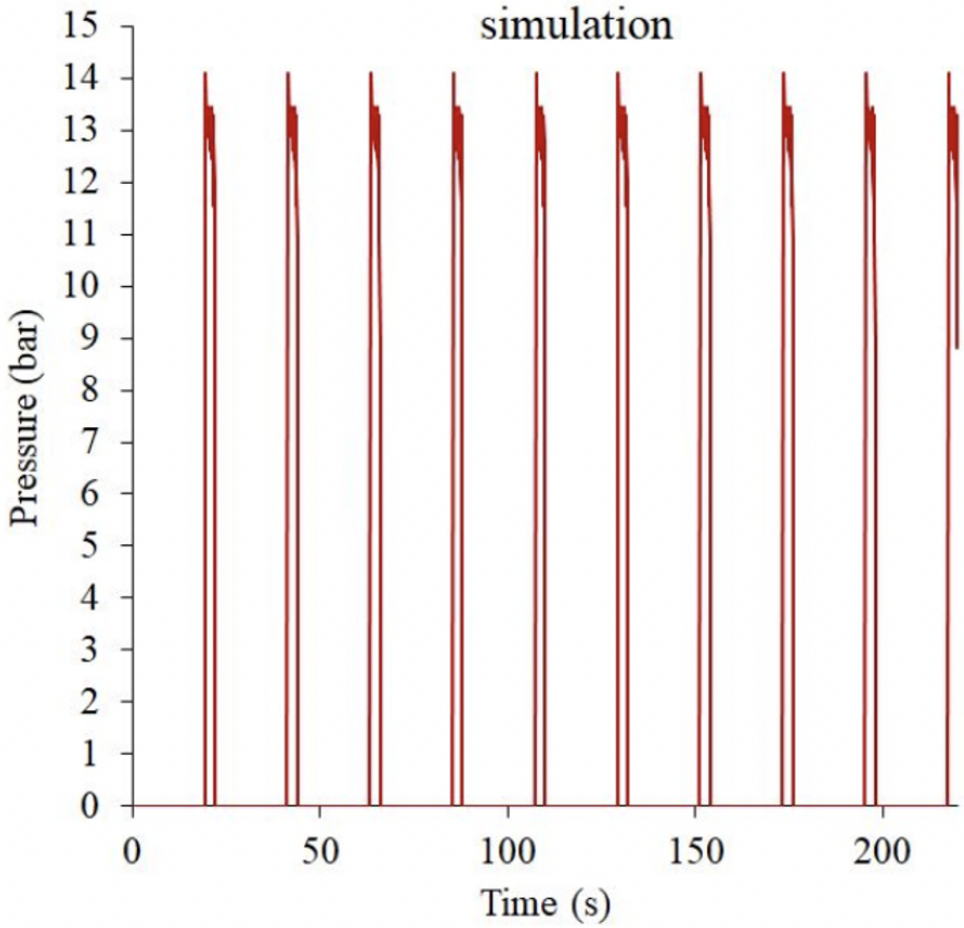

Figure 4.4: Contact pressures in simulated results.

The thermal model, like the aerodynamic model, provides information about the thermal behavior of the brake components that is difficult to observe with experiments. Figure 4.5 below shows the temperature distribution developed by friction on the disc during the simulation steps, starting from the 7th iteration. The heat generated by friction between the brake disc and the brake pad creates hotspot appearances on the disc. The maximum temperature on the disc occurs when the disc leaves the last section of brake pad in the direction of rotation. The heat generated here is dissipated during rotation by convection which is one of the heat transfer modes. As a result of convection, non-uniform temperature distribution was observed on the brake disc.

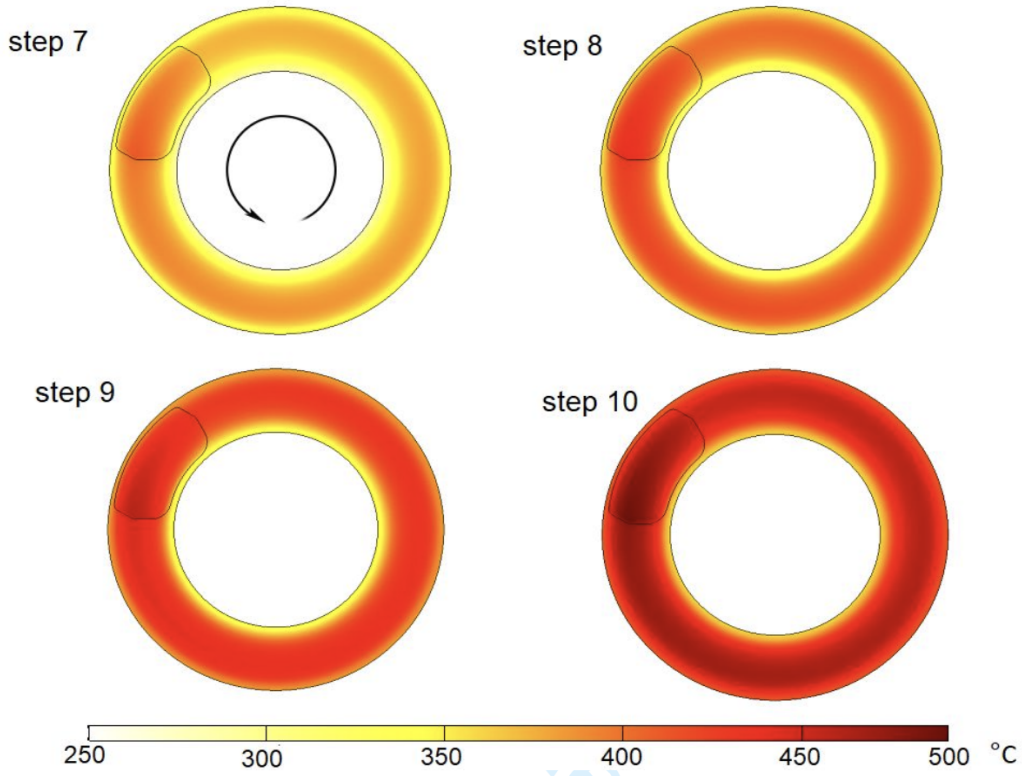

Figure 4.5: Temperature distribution on the rubbing surface of the disc at the end of cycles of 7 through 10.

Figure 4.6 shows the temperature distribution after the 10th braking sequence on the cut plane passing through the center of the simulated wheel. As shown in the figure, the highest temperature here is the contact area between the disc and pad. The temperature of this area was observed as 493 °C. The temperature of the region directly opposite the contact area is 461°C. These temperature measurements show that there is very low cooling during braking. The temperature of the air surrounding the disc and brake also increases due to the convection. Conduction, which is a type of heat transfer between solid parts, increases the temperature of the rim, hub and wheel to which the brake disc is connected up to 90°C. In the simulation, at the end of the 10th braking, the heat generated by friction is gradually dissipated into the atmosphere. The factor that causes this is the forced convection caused by the constant speed of 105 km/h air flow coming from the inlet of the computational domain.

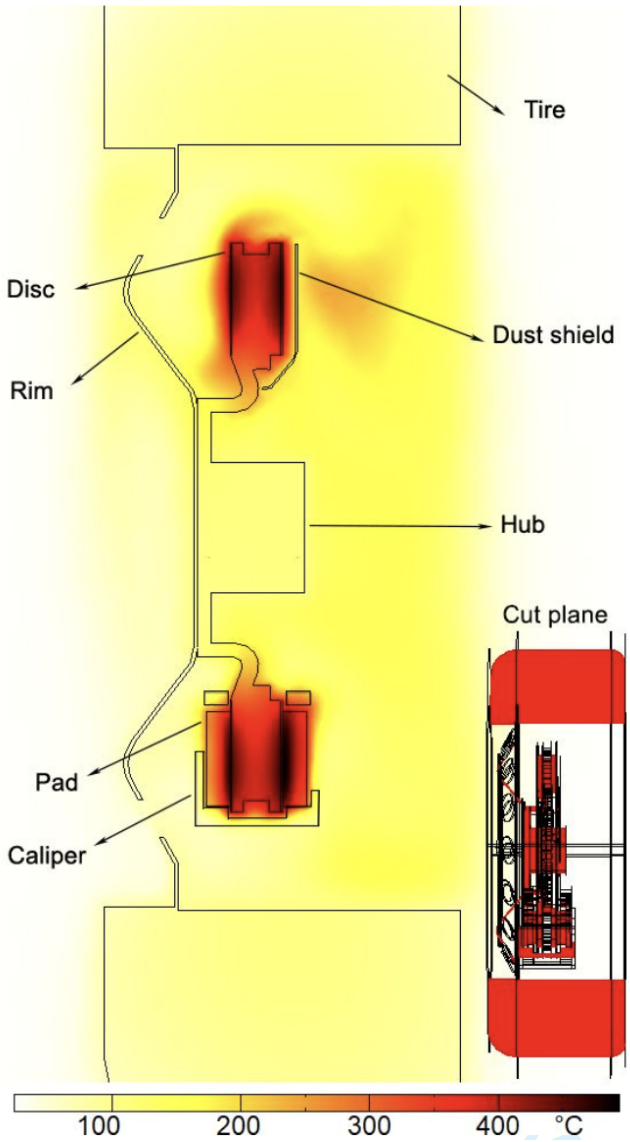

Figure 4.6: Temperature distribution on the cross-sectional view of the brake components at the end of tenth braking step.

The thermal model is not only made to show the temperature distribution, but also to analyze heat transfer modes and their magnitudes in total heat transfer. Figure 4.7 shows the trends of heat transfer modes for the braking during the cooling process. The dominant heat transfer mode in this process is forced convection. Convective heat transfer accounts for 88-93% of the entire heat transfer in the simulation. Another important point shown in this figure is the effect of the vanes in the disc on the cooling of the rotor.

The vanes in the disc cover 58-71% of the total convective heat transfer during the cooling phase. This data shows the importance of the vanes in the brake disc and their help on the cooling process. The conduction and radiation heat transfer modes constitute less than 10% of the total heat transfer.

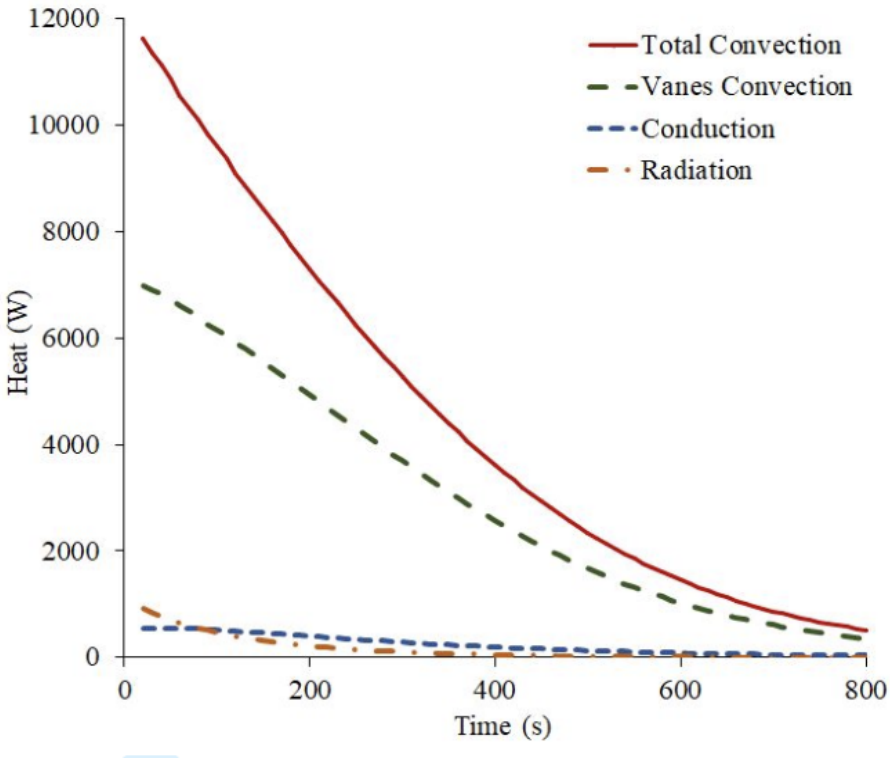

Figure 4.7: Effect of various Heat transfer modes for the braking process during the cooling step.

CHAPTER 5

EXPERIMENTAL SETUP

This section will concentrate on the experimental part of the work. In this section, the features of the experimental setup, how the measurements have been obtained and the test results are explained.

5.1 Features of Experimental Setup

The first step is the simulation part when examining the thermal and aerodynamic properties of brake systems. After the simulations are made, experiments are carried out to ensure the consistency and accuracy of the simulations with the real data.

The simulations provided thermal and aerodynamic data that could not be obtained or observed in experimental setups. The simulations were carried out under certain limits and conditions. The conditions and limits of the experimental setup should cover the conditions and limits of the simulation. Otherwise, the fact that the scenarios realized in the simulations cannot be tested in the experimental setup leads to the questioning of the consistency and accuracy of the study. Considering this rule, there must be a reciprocal relationship in the conditions and limits of simulations and experiments.

Since testing brake systems on a professional brake test dynamometer is expensive and time-consuming, a low-cost experimental setup that reflects the dynamics of braking has been produced. While the experimental setup was being produced, the braking scenario in which the brake test would be performed was determined first. In this scenario, it is desired to imitate the AMS hard braking brake test. Another determining factor is to determine which dimensions of a car the test samples will belong to. In this study, since the aim is to adapt the braking system of a full-size car on an experimental setup, the brake components are selected from the components used by a real car. Also, since the AMS brake tests were performed with a real car, an axial fan was included to imitate the air flowing around the brake components. This fan, which can operate at a maximum speed of 17 m/s, blows air to the brake components in the experimental setup. The speed of this fan can be adjusted via a frequency controller.

In the experimental setup, the frame to which the brake components will be connected was designed and fixed to the ground with bolts. The brake disc, caliper, pads, rim and tire are connected to the frame by the steering knuckle as in an automobile. A rotating shaft is connected to the frame with two ball bearings and one side of the shaft is coupled to the wheel and the other side to the AC motor which is the driving power.

Another feature of the experimental setup is the braking system mechanism used. Since the aim is to test a real brake system, the master cylinder, booster and pedal components in the brake system to be used were also used in the experimental setup.

In this experimental setup, an AC motor with a power of 2.2 kW was attached to the other end of the shaft with the wheel at one end and rotational movement of the test samples was ensured, since a drive power was required to imitate the movement of the wheel. In this experimental setup, flywheels that will imitate the inertia of the wheel and proportional to the weight of the car which are attached to the shaft.

In order to test the experimental setup on samples of different sizes, parts such as flywheel, master cylinder, booster, steering knuckle are designed to be removable and replaceable.

Figure 5.1 below shows the locations of the parts used in the setup, along with a schematic drawing of the experimental setup. The brake components used in this drawing and other equipment of the experimental setup are shown by naming.

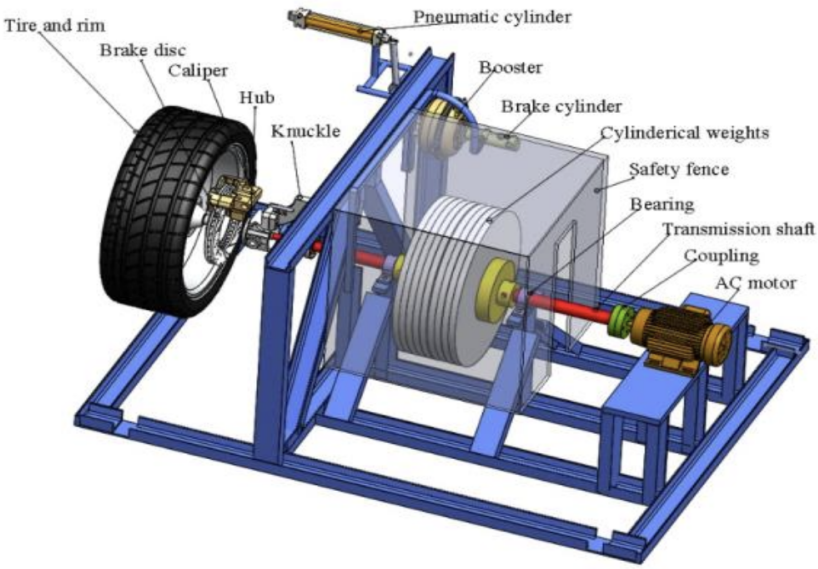

Figure 5.1: Schematic of experimental brake dynamometer.

5.2 Measurement and Control

In the previous section, the equipment used in the experiment setup and the working scenario of the setup are explained. Since the AMS hard braking test will be imitated in the experimental setup, it is desired to increase the rotational speed of the wheel to 105 km/h first and then to reduce the rotational speed to 0 km/h by hard braking. Since the first step of this scenario is to increase the wheel to 105 km/h, the AC motor that gives the driving force to the wheel must be controlled first. The rotational speed of the AC motor is controlled by an inverter. In order to assign the speed parameter to the frequency driver of the AC motor, first the wheel dimensions must be calculated.

Figure 5.2 below shows what the codes on the tire mean. In the next figure, 5.3, shows the code of the tire to be used in the dynamometer.

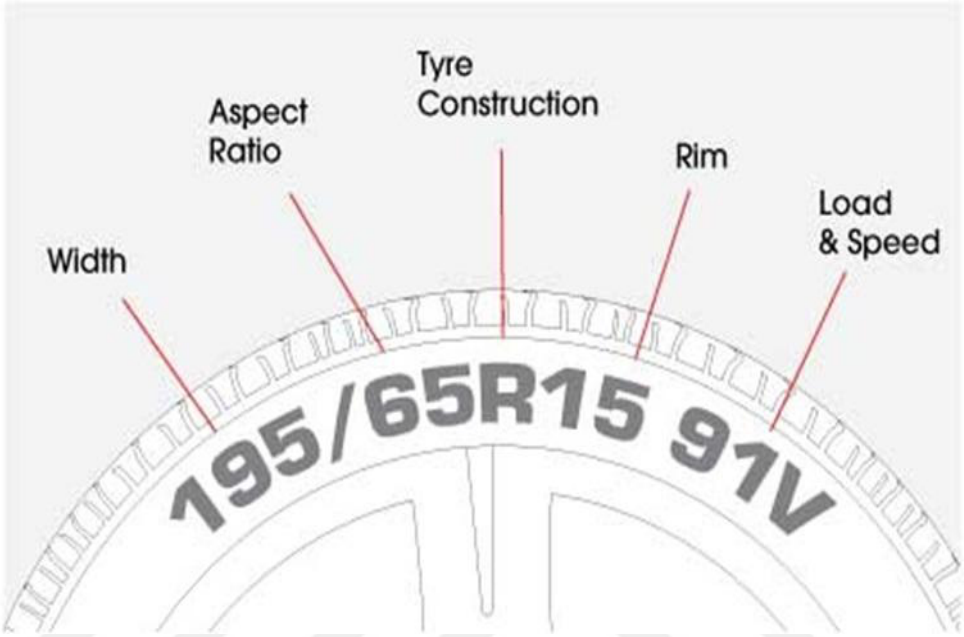

Figure 5.2: Tire codes explanations. Taken from Bridgestone (2022) [44]

Figure 5.3: Tire codes of the wheel on the experimental setup.

The radius of the wheel, which is calculated by the tire code in (Eqn. 5.1), is substituted into the circumference formula in (Eqn. 5.2). The distance traveled by a wheel with one full rotation is calculated. Since the aim in the planned AMS braking scenario is to increase the wheel to 105 km/h, the rpm value of the wheel at 105 km/h should be calculated. The wheel rpm value in (Eqn. 5.3) is converted to Hz in (Eqn. 5.4) below, which is the speed parameter of the AC motor, and the wheel speed is assigned to the frequency driver.

$$r_{wheel,\ in\ mm} = \frac{d_{rim,in\ inch}}{2} \cdot \frac{25.4\ mm}{1\ inch} + \ Wheel\ base\ x\ Aspect\ Ratio \qquad \text{(Eqn. 5.1)}$$

As a result of this operation, the r_{wheel} was calculated as 291.55 mm.

To calculate the distance traveled by the wheel;

$$P_{wheel} = r_{wheel}\ x\ \pi\ x\ 2 \quad \text{(Eqn. 5.2)}$$

The following Eqn. 5.3 is used to calculate ω_{wheel} at 105 km/h

$$\omega_{wheel} = v\ x\ \frac{1_{rev}}{P_{wheel}} \quad \text{(Eqn. 5.3)}$$

As a result of the calculation, the wheel reaches 105 km/h at 955.76 rpm.

In order to assign this rpm value to the frequency driver, this value must be calculated in Hz. This calculation is made in (Eqn. 5.4).

$$Hz = \frac{Rpm\ x\ Number\ of\ Poles}{120} \quad \text{(Eqn. 5.4)}$$

The calculated value of 31.8 Hz was assigned into the frequency driver of the AC motor.

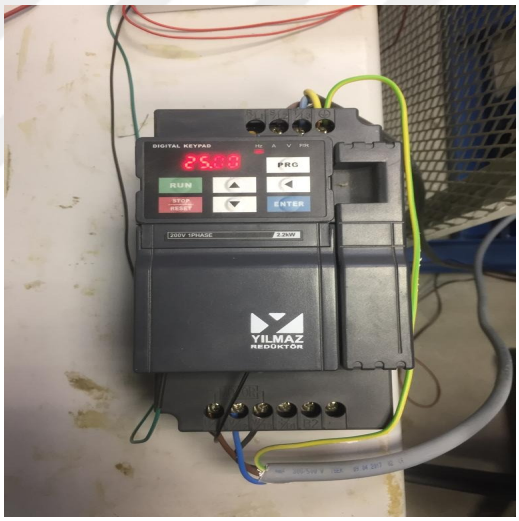

Figure 5.4: Frequency driver for AC motor control.

After the speed of the wheel is adjusted by programming the inverter, the braking status must be defined to the frequency driver. At the moment of braking, the inverter must stop the acceleration behavior. Otherwise, the wheel will continue to accelerate while braking. The inverter detects that the wheel has entered the braking state with the feedback from the rpm sensor on the AC motor. When the wheel reaches 955.76 rpm, the Arduino microcontroller sends a signal to the inverter. With this signal, the inverter stops the acceleration behavior of the wheel, and the braking process begins.

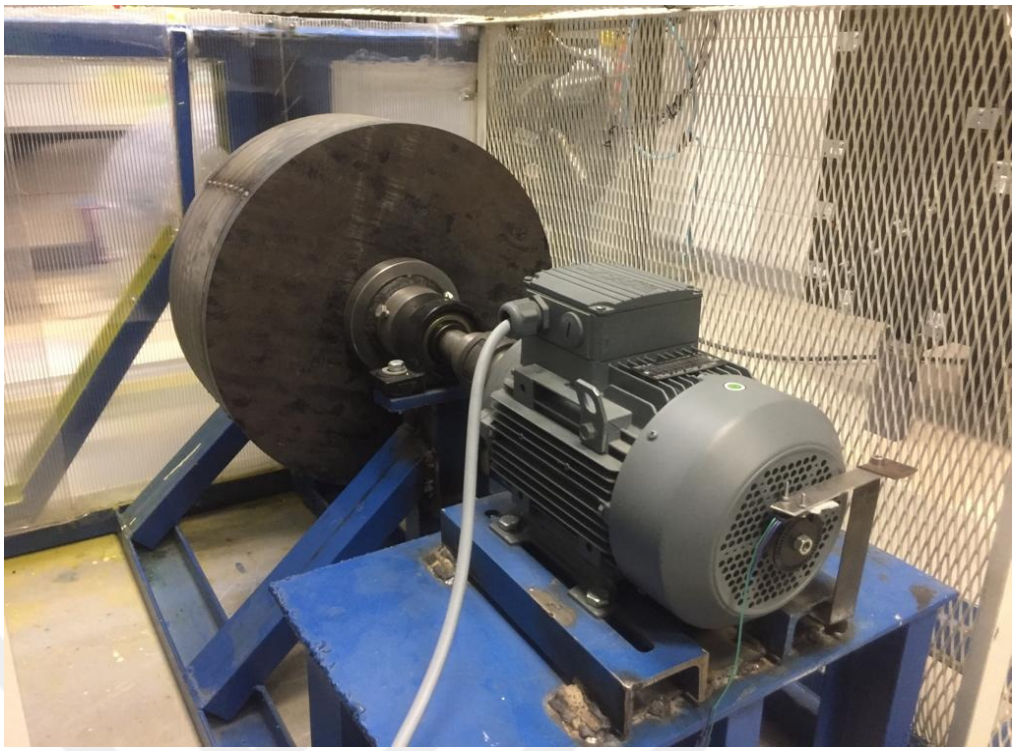

Figure 5.5: Rpm sensor, AC motor and flywheel on the shaft.

In the braking process, the Arduino microcontroller transmits the movement command to the pneumatic cylinder piston to perform braking with the rpm value signal coming from the rpm sensor. The air pressure of the piston is adjustable with the help of a one-way valve. The moving piston transmits the force to the brake booster with the help of a beam. In a real condition, an intake stroke of the engine is employed to create a vacuum for the booster to amplify the applied braking foot force. In the experimental setup, this vacuum required for this booster is produced by a small vacuum pump. The master cylinder to which the booster is connected is responsible for the pressure of the brake fluid.

The pressure from the master cylinder is transmitted to the brake caliper through the brake fluid pipes, and the brake pads are pressed against the disc by the piston mechanism in the caliper. Thus, the chain reaction of the braking situation was started with only a single rpm data.

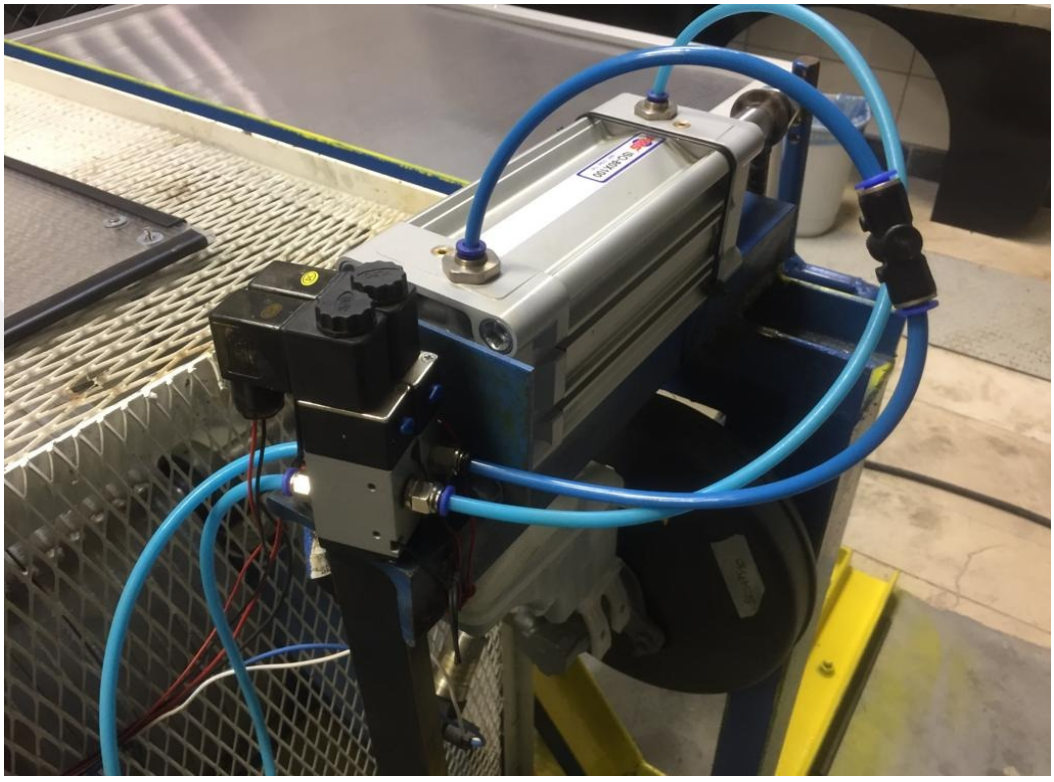

Figure 5.6: Pneumatic piston that creates the braking force and pneumatic valves on the side.

After the motion and braking behaviors are adjusted, the test specimens will run in acceleration and braking cycles for the desired number of repetitions. After the cycle is established, data should be collected on the test samples. The data to be collected at this stage has been determined beforehand. These are the temperature of the brake disc-pad and the contact pressure between the disc and the brake pad.

K-type thermocouples were used to collect the temperature data. The easiest and most common way to measure the temperature on a rotating disc is rubbing thermocouple.

The second data that needs to be collected is the contact pressure between the brake disc and the brake pad. This pressure was measured with a pressure transducer (FOX TR42X.2) connected to the master cylinder.

Since thermocouple and pressure transmitter measures the data by sending signals. To convert these signals into meaningful expression, a data acquisition device is required. In this study, Agilent Benchlink 34972A device recorded the signals from thermocouple and pressure transmitter every 0.5 seconds.

Figure 5.7: Rubbing thermocouple on brake disc.

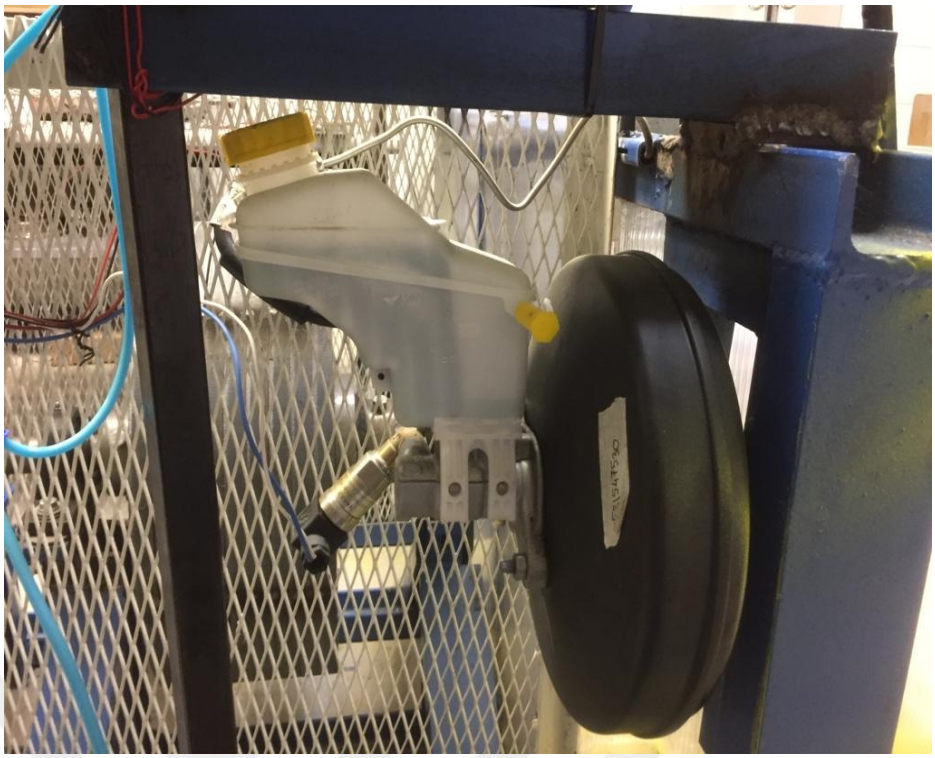

Figure 5.8: Master cylinder, booster, brake fluid reservoir and pressure transducer.

Figure 5.9: Test rig while accelerating the brake components.

5.3 Experiment Results

The data collected as a result of the experiments on the brake mechanism were processed in the data acquisition device. The data is processed in the form of graphs in order to compare them with the values in the simulations.

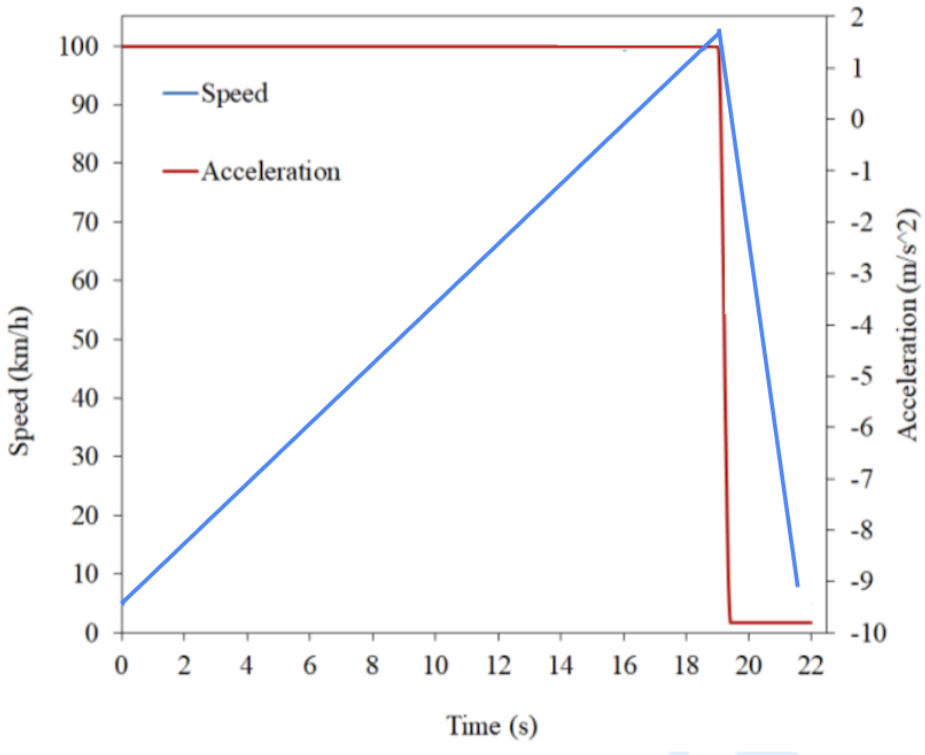

Figure 5.10 Acceleration and Speed Changes in one braking.

The level of G-forces experienced during a panic braking event can vary greatly depending on several factors, including the initial speed of the vehicle, the rate of deceleration, and the size and weight of the vehicle. In general, panic braking can generate G-forces ranging from 0.5 G to over 2 G. For example, in a panic stop from 60 mph (97 km/h), a typical passenger car may experience G-forces of around 0.9 G.

In the experimental setup, dynamometers braking behavior adjusted for this circumference. Figure 5.10 shows the acceleration-deceleration and speed variation of the dynamometer in one braking step. The braking characteristic of experimental setup shows that while braking occurs braking components decelerates around 0.9 G.

The figure below 5.11 shows the brake pressure applied in the experiment setup. At high pressure moments, the pressure value changed by 2 bars. Besides, the pressure value measured in the experimental setup agrees very well with the value measured in the simulation. In the experimental setup, the peak values of the pressure vary slightly between steps, this is due to the variability of the pressure of the compressed air inside the pneumatic piston used for braking.

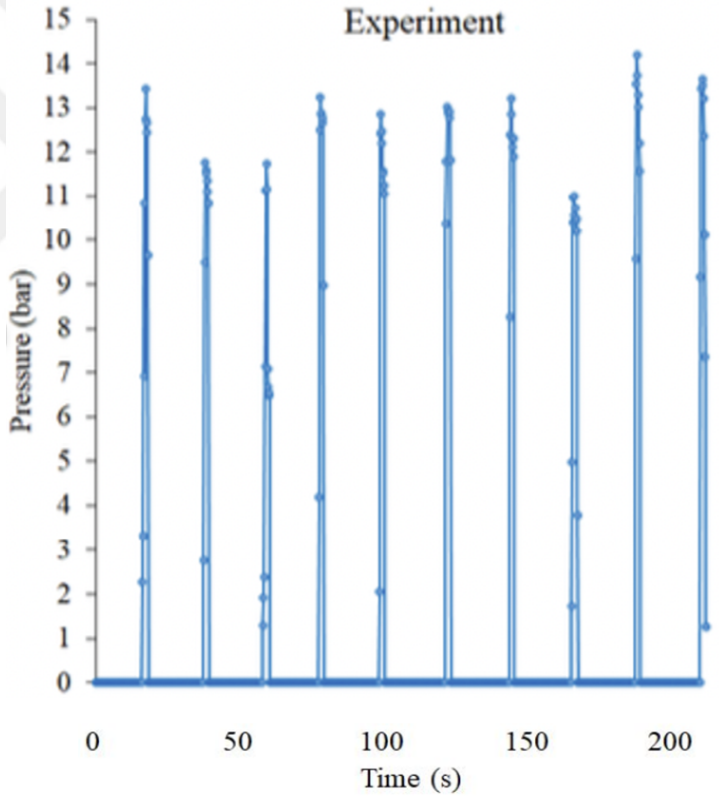

Figure 5.11: Contact pressures measured in the experiment.

Another value measured in the experiment setup is the temperature data on the disc that develops as a result of the friction of the brake disc and pad. The figure 6.2 below in VALIDATION chapter shows the temperature of the brake disc rubbing against the pad, comparing it to the simulation temperatures. In this study, since the speed of the blowing fan used to create air flow on the brake components is limited to 17m/s, the results are predicted. The over prediction here increases as the braking sequences proceed. The predicted temperature values for the cooling stage were lower than the simulation.

5.4 Uncertainty Analysis of Experiments

The J type thermocouple probe accuracy is 1.1°C. In addition, switching, conversion, and reference junction errors are already included in the measurement specification of the data acquisition and equals to 1°C. Total uncertainty is then 2.1 °C. Used FOX TR42X.2 pressure transducers error is < 1% at 20°C due to its datasheet. Total uncertainty is 0.11- 0.14 bar between the experiment steps; these values also include data acquisition device AC current measurement errors.

CHAPTER 6

VALIDATION

One of the important aspects of an academic study is to prove the accuracy of the calculated values in numerical simulations and their consistency with experimental data. In this context, the validity of the study was proven by comparing the consistency of the thermal and aerodynamic simulations with the experimental data.

The accuracy of the thermal simulation is shown in figure 6.1 below by comparing the contact pressure value obtained in thermal simulations with the contact pressure value in the experiment.

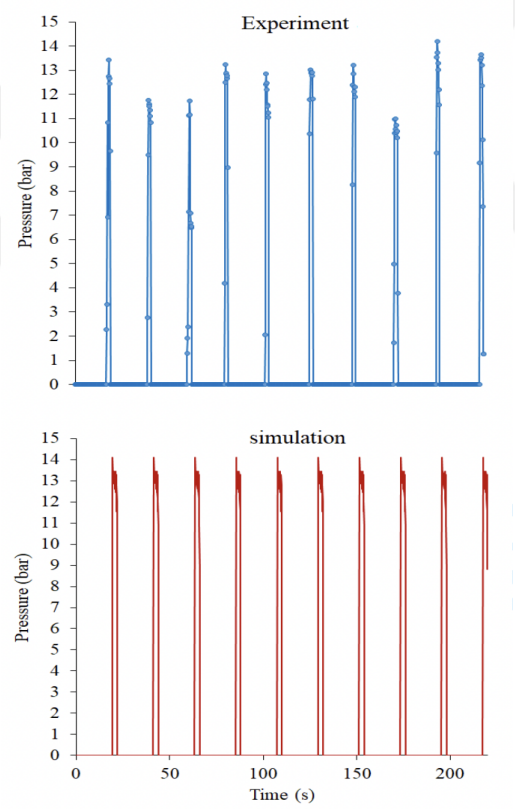

Figure 6.1: Comparison of Contact pressure variation between experiment and numerical simulation.

It is observed that the simulation and experiment values shown in Figure 6.1 are in good agreement. The relationship of contact pressure with simulation and experiments has been described in previous chapters.

Another data used to verify the consistency of the experiments with numerical simulations is the temperature values after the friction state of the brake disc. Figure 6.2 below is used to make this comparison.

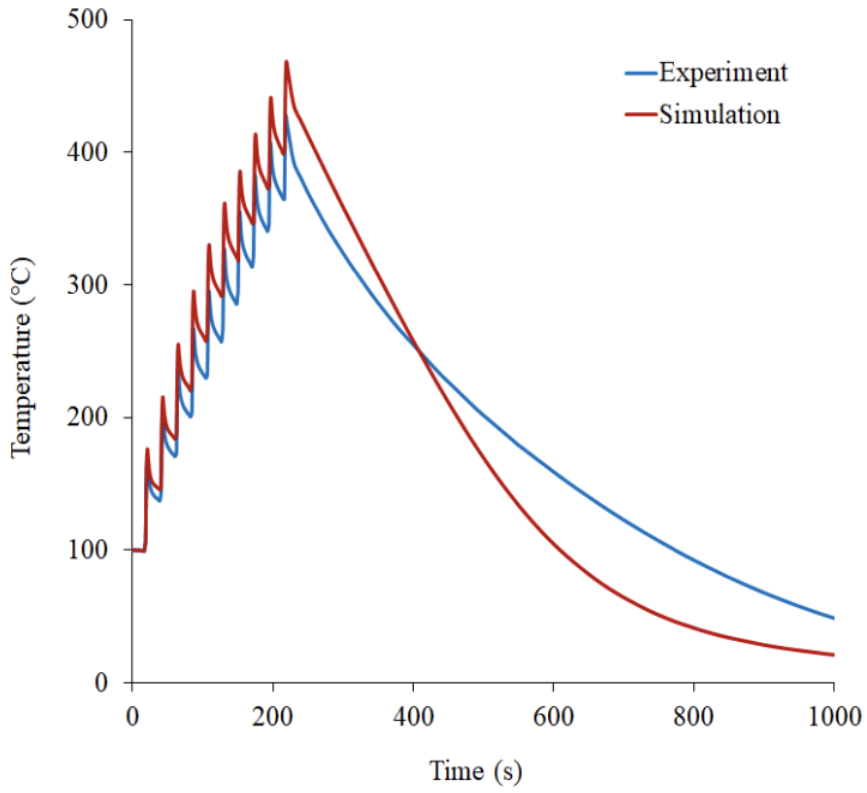

Figure 6.2: Comparison of the temperature variation between the experiment and numerical simulation for ten sequential braking steps and cooling step.

CHAPTER 7

CONCLUSION

In this master's thesis, first, the components and working principles of the brake system were introduced with the determined purpose. Then, the tests that the brake system components are subjected to are explained. The aim of this study is to design and manufacture an experimental setup to prove the accuracy of simulations, as well as which thermal and aerodynamic analyses of brake components will be performed on a full-size brake system.

In the literature review, it was observed how the previous studies were carried out and what kind of methods they followed to prove the accuracy of their studies. Inspired by studies in the literature, a brake testing methodology was developed in this study to test a full-size brake system. In this methodology, firstly, a numerical model is built. Under the numerical model, geometric modeling, aerodynamic model, and thermal model were planned and simulations were carried out. Geometric models were obtained by modeling a full-size brake system part in one-to-one ratio. Later, these models were assigned to simulations and thermal and aerodynamic simulations were carried out on them.

In the aerodynamic simulations, the behavior of the air flow over the brake components is simulated in the CFD program Comsol Multiphysics, and the turbulent air flow around the brake components is modeled. It has been observed in this model that the speed of air flow in the rim is much lower than the speed of movement of the car. The low velocity air flow in the wheel causes eddy formations around the brake components. These eddy formations cause the heat to arise from the friction between the disc and the pad to be transmitted to other components by convection. The purpose of making the thermal model is to show the percentage distribution of the heat transfer modes on brake components. In addition, the contribution of the vents in the brake disc to the cooling performance on the brake rotor has been observed.

The thermal simulation values show the temperature distribution over the brake components. It has been understood from the simulations that hot spots occur on the disc. The highest temperature measured in the components is 493°C, measured at the point where the brake disc leaves the brake pad in rotational motion. At the opposite point on the contact area the temperature was observed as 461°C. The following deduction can be made easily from here; the brake disc shows a slight cooling behavior as soon as it leaves the contact point. This prevents the uniform distribution of the temperature. The percentage distribution of heat transfer mechanisms obtained through thermal simulations shows that the heat generated by friction in the brake system is mostly dissipated by convection. In addition, the channels in the radial ventilated brake disc helped the forced convection due to airflow and dissipated the heat in the brake disc with convection in the range of 58-71%. These obtained values present different results than the values researched in the literature. Vdovin calculated this value as 53% in his study. Shuetz, on the other hand, estimated the cooling of the ventilated brake disc as 63.4% in his experiments at 140 km/h.

In order to ensure the accuracy and consistency of the simulations, a brake dynamometer is manufactured. Since the brake components in the manufactured brake dynamometer will be the same as in an automobile, the components have been chosen in full size. After the braking system was assembled to a frame with all its components, a control system suitable for the AMS hard braking scenario was developed. This scenario is of a repetitive cyclical structure and the brake components were first accelerated to 105 km/h as in the car, and then their speed was reduced to zero again with hard braking. The little detail that lies here is why it is 105 km/h, not exactly 100 km/h. The reason for this is the flywheel, which imitates the weight of the car in the brake test experimental setup. Since the acceleration of the motor used in the experimental setup takes time, cooling of the brake disc has occurred between the sequences. As a solution to this problem, the brake components were reduced to 5 km/h instead of 0 km/h at the end of the braking sequence. Therefore, the speed of the components has been increased to 105 km/h. Another limiting factor in the

experimental setup is the airflow that develops due to the speed of the car in the AMS brake test. In order to imitate this situation in the experimental setup, a blowing fan was placed in front of the wheel. However, the speed of this fan is limited to 17 m/s.

For this reason, while the cooling behavior is observed after the braking sequences, there is a difference between the values obtained in thermal simulations. Although this difference is tried to be reduced through prediction, it affects the results of the experiment.

After the experiments to validate the simulations, the consistency between the simulation results and the experiments was observed. For accuracy, the friction coefficient, contact area and the rotational speed of the components must be known, but these values are already the same in the simulation and in the experimental setup. At this point, two parameters come to the fore in order to determine the consistency between the experimental setup and the simulation. The first of these is the contact pressure. As expressed in the numerical model, the contact pressure is proportional to the heat produced by friction. The second is the temperature of the brake disc. According to the data obtained, these parameters measured in simulation and experiments showed consistency between them. In the light of these data, the accuracy of this study has been proven.

CHAPTER 8

FUTURE WORK

A lot of study has been done on brake components so far and work in this area will continue in the future. In today's world, electric cars are replacing internal combustion cars. If we look at this situation through brake systems, the performance of brake systems has an important place in the automotive industry. Electric cars are heavy due to the battery. For this reason, the force required to stop or slow down the vehicle will be increased. For this reason, heat management in brake components is important. At the same time, the importance given to the environment is gradually increasing due to climatic conditions. The particles that break off from the brake pads create an emission, no matter how environmentally friendly they are produced.

Besides simulations, the experimental setup can be modified for different brake tests. While this thesis was being written, in a study carried out on the experimental setup, the particles of the brake pad were collected after an isolated environment was created around the disc and pad.

As another future work, redesigning the structures of the channels in the brake discs so that they can perform more efficient cooling should be considered. In this study, ventilation channels in the brake disc showed a benefit in the range of 58-71% for cooling the brake disc. Rather than testing a single disc on the models of brake discs, many variations of brake disc models can be tested with this experimental setup and simulation models.

In addition, turbulent flow was observed in the wheel in this study. Rim designs that will affect the behavior of this developing turbulent air flow can also be tested in this experimental setup, and a more effective cooling behavior on brake components can be investigated.

REFERENCES

[1] “Brake System Guide.” Internet: www.bendix.com.au/help/the-bendix-brake-system-guide-an-intro-to-bendix-disc-brake-function-and-maintenance, Accessed [2022].

[2] D. J. Purdy, D. Simner, D. Diskett, A. Duncan, P. J. H. Wormell, and C. Stonier, “An experimental and theoretical investigation into the roll-over of tracked vehicles,” *Proceedings of the Institution of Mechanical Engineers, Part D: Journal of Automobile Engineering*, vol. 230, no. 3, pp. 291–307, May 2015

[3] Maleque, M. A., S. Dyuti, and M. M. Rahman, "Material selection method in design of automotive brake disc," *Proceedings of the world congress on engineering*, 2010, pp. 2322-2326.

[4] “Brembo Official Website.” Internet: www.brembo.com/en/car/original-equipment/products/discs, Accessed [2022].

[5] “HELLA PAGID Official Website.” Internet: www.hella-pagid.com/hellapagid/en/Copper-free-brake-pads-613.html, 22 June 2018, Accessed [2022].

[6] Chan, D. S. E. A., and G. W. Stachowiak. "Review of automotive brake friction materials." *Proceedings of the Institution of Mechanical Engineers, Part D: Journal of Automobile Engineering*, vol. 218, no. 9, pp. 953-966, 2004.

[7] “Automotive Braking Trends.” Internet: www.lapinus.com/applications/automotive/our-thinking/automotive-braking-trends-the-inside-track, Accessed [2022].

[8] “Automobile - Brakes.” Internet: www.britannica.com/technology/automobile, Accessed [2022].

[9] T. D. Mew, K.-J. Kang, F. W. Kienhöfer, and T. Kim, “Transient thermal response of a highly porous ventilated brake disc,” *Proceedings of the Institution of Mechanical Engineers, Part D: Journal of Automobile Engineering*, vol. 229, no. 6, pp. 674–683, Jan. 2015.

[10] A. Coulibaly, N. Zioui, S. Bentouba, S. Kelouwani, and M. Bourouis, “Use of thermoelectric generators to harvest energy from motor vehicle brake discs,” *Case Studies in Thermal Engineering*, vol. 28, p. 101379, Dec. 2021.

[11] R. Jafari and R. Akyüz, “Optimization and thermal analysis of radial ventilated brake disc to enhance the cooling performance,” *Case Studies in Thermal Engineering*, vol. 30, p. 101731, Feb. 2022.

[12] “Brake Testing for Third Parties - TecSA R&D Laboratory.” Internet: www.tecsa-srl.it/en/brake-testing-for-third-parties, Accessed [2022].

[13] David Eggleston, “An investigation into frictional surface interactions and their effect on brake judder,” PhD Thesis, Sheffield Hallam University, United Kingdom, 2000.

[14] S. Bilgic Istoc and H. Winner, “Heat cracks in brake discs for heavy vehicles,” *Automotive and Engine Technology*, vol. 3, no. 1–2, pp. 61–68, Apr. 2018.

[15] A. Vdovin and G. Le Gigan, “Aerodynamic and Thermal Modelling of Disc Brakes—Challenges and Limitations,” *Energies*, vol. 13, no. 1, p. 203, Jan. 2020.

[16] Schuetz, Thomas, “Cooling analysis of a passenger car disk brake,” *SAE Technical Paper*, No. 2009-01-3049, 2009.

[17] A. Vdovin, M. Gustafsson, and S. Sebben, “A coupled approach for vehicle brake cooling performance simulations,” *International Journal of Thermal Sciences*, vol. 132, pp. 257–266, Oct. 2018.

[18] Pevec, M., et al. "Prediction of the cooling factors of a vehicle brake disc and its influence on the results of a thermal numerical simulation." *International Journal of Automotive Technology*, vol. 13, no. 5, pp. 725-733, 2012.

[19] Yan, H., et al. "Experimental and Numerical Study of Turbulent Flow and Enhanced Heat Transfer by Cross-Drilled Holes in a Pin-Finned Brake Disc." *International Journal of Thermal Sciences*, vol. 118, pp. 355-366, 2017.

[20] Q. Jian and Y. Shui, “Numerical and experimental analysis of transient temperature field of ventilated disc brake under the condition of hard braking,” *International Journal of Thermal Sciences*, vol. 122, pp. 115–123, Dec. 2017.

[21] K. Stevens and M. Tirovic, “Heat dissipation from a stationary brake disc, Part 1: Analytical modelling and experimental investigations,” *Proceedings of the Institution of Mechanical Engineers, Part C: Journal of Mechanical Engineering Science*, vol. 232, no. 9, pp. 1707–1733, May 2017.

[22] A. A. Yevtushenko, M. Kuciej, and E. Och, “Temperature in thermally nonlinear pad–disk brake system,” *International Communications in Heat and Mass Transfer*, vol. 57, pp. 274–281, Oct. 2014.

[23] A. Yevtushenko and P. Grzes, “Maximum temperature in a three-disc thermally nonlinear braking system,” *International Communications in Heat and Mass Transfer*, vol. 68, pp. 291–298, Nov. 2015.
[24] P. Grzes, W. Oliferuk, A. Adamowicz, K. Kochanowski, P. Wasilewski, and A. A. Yevtushenko, “The numerical–experimental scheme for the analysis of temperature field in a pad-disc braking system of a railway vehicle at single braking,” *International Communications in Heat and Mass Transfer*, vol. 75, pp. 1–6, Jul. 2016.

[25] P. Hwang and X. Wu, “Investigation of temperature and thermal stress in ventilated disc brake based on 3D thermo-mechanical coupling model,” *Journal of Mechanical Science and Technology*, vol. 24, no. 1, pp. 81–84, Jan. 2010.

[26] G. Le Gigan, T. Vernersson, R. Lundén, and P. Skoglund, “Disc brakes for heavy vehicles: an experimental study of temperatures and cracks,” *Proceedings of the Institution of Mechanical Engineers, Part D: Journal of Automobile Engineering*, vol. 229, no. 6, pp. 684–707, Oct. 2014.

[27] L. Qiu, H.-S. Qi, and A. Wood, “Two-dimensional finite element analysis investigation of the heat partition ratio of a friction brake,” *Proceedings of the Institution of Mechanical Engineers, Part J: Journal of Engineering Tribology*, vol. 232, no. 12, pp. 1489–1501, Feb. 2018.

[28] O. I. Abdullah, J. Schlattmann, M. H. Majeed, and L. A. Sabri, “The temperatures distributions of a single-disc clutches using heat partitioning and total heat generated approaches,” *Case Studies in Thermal Engineering*, vol. 11, pp. 43–54, Mar. 2018.

[29] G. P. Voller, M. Tirovic, R. Morris, and P. Gibbens, “Analysis of automotive disc brake cooling characteristics,” *Proceedings of the Institution of Mechanical Engineers, Part D: Journal of Automobile Engineering*, vol. 217, no. 8, pp. 657–666, Aug. 2003.

[30] Hwang, Pyung, Xuan Wu, and Young-Bae Jeon. "Thermal-mechanical coupled simulation of a solid brake disc in repeated braking cycles." *Proceedings of the Institution of Mechanical Engineers, Part J: Journal of Engineering Tribology*, vol. 223, no. 7, pp. 1041-1048, 2009.

[31] Stojanović, Nadica R., et al. "Pressure influence on heating of ventilating disc brakes for passenger cars." *Part A: Thermal Science*, vol 24, no 1, pp 203-214, 2020.

[32] Galindo-Lopez, Carlos Hannover. “Optimisation of convective heat dissipation from ventilated brake discs,” PhD Thesis, Cranfield University, United Kingdom, 2009.

[33] A. Modanloo and M. R. Talaee, “Analytical thermal analysis of advanced disk brake in high speed vehicles,” *Mechanics of Advanced Materials and Structures*, vol. 27, no. 3, pp. 209–217, May 2018.

[34] Q. Jian, L. Wang, and Y. Shui, “Thermal analysis of ventilated brake disc based on heat transfer enhancement of heat pipe,” *International Journal of Thermal Sciences*, vol. 155, p. 106356, Sep. 2020.

[35] D. Meresse, S. Harmand, M. Siroux, M. Watremez, and L. Dubar, “Experimental disc heat flux identification on a reduced scale braking system using the inverse heat conduction method,” *Applied Thermal Engineering*, vol. 48, pp. 202–210, Dec. 2012.

[36] A. A. Alnaqi, D. C. Barton, and P. C. Brooks, “Reduced scale thermal characterization of automotive disc brake,” *Applied Thermal Engineering*, vol. 75, pp. 658–668, Jan. 2015.

[37] A. Sellami, M. Kchaou, R. Elleuch, and Y. Desplanques, “Thermal analysis of pad-on-disc contact under tribological solicitations: a coupled numerical–experimental approach to identify surface temperatures and flow partition coefficient,” *Heat and Mass Transfer*, vol. 52, no. 9, pp. 1923–1934, Nov. 2015.

[38] L. Qiu, H.-S. Qi, and A. Wood, “Two-dimensional finite element analysis investigation of the heat partition ratio of a friction brake,” *Proceedings of the Institution of Mechanical Engineers, Part J: Journal of Engineering Tribology*, vol. 232, no. 12, pp. 1489–1501, Feb. 2018.

[39] Neys, Adriaan, “In-vehicle brake system temperature model.” MSc thesis, Chalmers University of Technology, Sweden, 2012.

[40] Pulugundla, Gautam, "CFD design analysis of ventilated disc brakes." MSc thesis, Cranfield University, United Kingdom, 2008.

[41] Thuresson, Adrian. “CFD and Design Analysis of Brake Disc.” MSc thesis, Chalmers University of Technology, Sweden, 2014.

[42] Bergman, Theodore L., *Introduction to heat transfer*, Hoboken, New Jersey: John Wiley & Sons, 2011, p 381.

[43] M. G. Cooper, B. B. Mikic, and M. M. Yovanovich, “Thermal contact conductance,” *International Journal of Heat and Mass Transfer*, vol. 12, no. 3, pp. 279–300, Mar. 1969.

[44] “Understanding Tyre Sizes.” Internet: www.bridgestone.com.au/learn/understanding-tyre-sizes, Accessed [2022]